EVALUATION OF STRUCTURAL STRENGTH CHARACTERISTICS OF LIGHT POLE TRANSFORMER BASES

PB98-148943

Prepared by:

C.V. Girija Vallabhan, William Burkett,
Adinarayana S. Mukkamala, Md. Monirul Haque
Ritesh Kumar
Dept. of Civil Engineering
Texas Tech University
Lubbock, TX 79409

Submitted to:

Texas Department of Transportation

October 1998

Research Study No: 0-1416

REPRODUCED BY: NTIS
U.S. Department of Commerce
National Technical Information Service
Springfield, Virginia 22161

TECHNICAL DOCUMENTATION PAGE

1. Report No. 1416-1R	2. Government Accession No.	3. Recipient's Catalog No.
4. Title and Subtitle Evaluation of Structural Strength Characteristics of Light Pole Transformer Bases		5. Report Date October 1997 6. Performing Organization Code
7. Author(s) C.V.Girija Vallabhan, William R. Burkett Tony Mollhagen, Matt Evans, Thomas Lehman		8. Performing Organization Report No.
9. Performing Organization Name and Address Department of Civil Engineering Texas Tech University Lubbock, TX 79409-1023		10. Work Unit No. (TRAIS) 11. Contract or Grant No. 0-1416
12. Sponsoring Agency Name and Address Texas Department of Transportation P.O. Box 5080 Austin, TX 78763-5080		13. Type of Report and Period Covered Final Report Sept 1995 - Aug 1997 14. Sponsoring Agency Code
15. Supplementary Notes		

16. Abstract:

Brittle cast aluminum transformer bases used as breakaway supports for luninaire poles to protect occupants during vehicular collisions, must also resist moments caused by lateral wind loads. To study its moment capacity, a three dimensional finite element model using CSA/NASTRAN was developed for analyzing both TBI-17 and TB3-17 t-base models. To validate the finite element results, full scale tests were conducted. The behavior of the t-base/ light pole system is a complex interaction which is affected by properties of the t-base, base plate thickness, diameters of the bolt circles at the top and bottom of the t-base. Critical loading orientations of the t-base were investigated and determined. The material properties of the cast aluminum, such as modulus of elasticity, ultimate tensile strength, rockwell hardness number were investigated, by testing specimens cut from the t-bases. Also, an attempt was made to correlate the material properties with the ultimate moment capacity of the t-base. For the use of field engineers, a simple interpolation computer program was developed, to determine the ultimate moment of transformer base/steel base plate system by inputting the actual base plate thickness, bolt circle diametrs, t-base used and the steel pole diameter.

17. Key Words Breakaway Transformer Base, T-base, Light Pole, Base Plate, Finite Element Analysis, aHardness, Tensile Strength, Ultimate Moment Capacity, Wind Loading, Full scale tests.		18. Distribution Statement No restrictions. This document is available to the public through the National Technical Information service, Springfield, Virginia 22161	
19. Security Classif. (of this report) Unclassified	20. Security Classif. (of this page) Unclassified	21 74	22. Price

Form DOT F 1700.7 (8-72) Reproduction of completed page authorized

IMPLEMENTATION STATEMENT

Numerical finite element analysis and experimental work have been completed as proposed to validate the conclusions made in this report. Through a interpolation computer program, the ultimate moment capacity of the t-base / steel base plate system can be determined for the values of parameters in between the limiting values reported here.

Dissemination of this information can be accomplished through the Traffic Operations Division, TxDOT.

AUTHOR'S DISCLAIMER

The contents of this report reflect the views of the authors who are responsible for the facts and the accuracy of the data presented herein. The contents do not necessarily reflect the official view of policies of the Department of Transportation or the Federal Highway Administration. This report does not constitute a standard, specification, or regulation.

PATENT DISCLAIMER

There was no invention or discovery conceived or first actually reduced to practice in the course of or under this contract, including any art, method, process, machine, manufacture, design or composition of matter, or any new useful improvement thereof, or any variety of plant which is or may be patentable under the patent laws of the United States of America or any foreign country.

ENGINEERING DISCLAIMER

Not intended for construction, bidding, or permit purposes. The engineer in charge of the research study was Warren K. Wray, P.E., Texas 51199.

TRADE NAMES AND MANUFACTURERS' NAMES

The United States Government and the State of Texas do not endorse products or manufacturers. Trade or manufacturers' names appear herein solely because they are considered essential to the object of this report.

TABLE OF CONTENTS

TECHNICAL DOCUMENTATION ii
IMPLEMENTATION STATEMENT iii
AUTHOR'S DISCLAIMER iii
TRADE NAMES AND MANUFACTURES'S NAMES iii
ACKNOWLEDGEMENTS iii

CHAPTER

1. INTRODUCTION 1
   1.1 Overview 1
   1.2 Functionality of the T-Base 1
   1.3 Problem Statement 1
2. REVIEW OF PAST RESEARCH 4
3. RESEARCH APPROACH 5
   3.1 Variability in the Material 5
   3.2 Critical Load Orientation of the T-Base 5
   3.3 Controlling Parameters or Dimensions During Fixing a T-Base 5
   3.4 A Simple Computer Code for Strength of a T-Base System 6
   3.5 Recommendations and Guidelines 6
4. CRITICAL LOAD ORIENTATION 7
   4.1 Introduction 7
   4.2 Loading Orientations 7
   4.3 Finite Element Modeling 9
   4.4 Comparison of Stresses and Displacements in Different Loading Orientations 11
   4.5 Discussion of Results 11
5. EXPERIMENTAL SETUP AND PARAMETRIC STUDY 14
   5.1 Experimental Procedure to Determine the Structural Strength of the T-Base 14
      5.1.1 Introduction 14
      5.1.2 Test Frame Representing Concrete Pier Foundation 14
      5.1.3 T-Base/Light Pole Setup 14
      5.1.4 Load Bar Calibration 16
      5.1.5 Key Dimensional Parametric Study 16
      5.1.6 Test Plan 19
      5.1.7 Test Procedure 19
   5.2 Experimental Results 22
      5.2.1 Experimental Results 22
      5.2.2 T-base failure location 22
   5.3 Determination of Material Properties of T-base 31
      5.3.1 Preparation of Tension Test Specimens 31

5.3.2 Test Procedure 32
5.3.3 Results of Material Properties from Tension Tests 32
5.3.4 Rockwell Hardness Test 32
5.3.5 Test Procedure 32
5.3.6 Results of Hardness Tests 34
6. VALIDATION OF FINITE ELEMENT MODEL 35
6.1 Introduction 35
6.2 Modeling of Part of Light Pole 35
6.3 Thickness of T-Base Shell 37
6.4 Contact Surfaces Not Welded Within the T-Base 37
6.5 Modeling of Side Opening (Door) 37
6.6 Validation of Finite Element Results 38
6.7 Comparison of Strains with Experiments 38
6.7.1 Comparison of Strains in the Base Plate 38
6.7.2 Comparison of Strains in the T-Base 41
6.8 Nonlinear Behavior of the T-Base and the Base Plate 46
6.9 Validation and Calibration of Finite Element Models 46
7. CORRELATION OF FEM WITH EXPERIMENTS 48
7.1 Introduction 48
7.2 Effect of Top Bolt Circle 48
7.3 Effect of Bottom Bolt Circle 51
7.4 Effect of Base Plate Thickness 52
7.5 Effect of Pole Diameter 53
7.6 Interaction Effect of Key Dimensional Parameters 53
7.7 Strength Comparison of 1975 and 1985 AASHTO Standard T-Bases 54
7.8 Quality Control Study 59
7.9 Effect of Leveling Devices 60
8. COMPUTER CODE FOR MOMENT CAPACITIES 61
8.1 Introduction 61
8.2 Interpolation of Ultimate Moment Capacities 61
8.3 Computer Code 61
9. CONCLUSIONS AND RECOMMENDATIONS 62
9.1 Conclusions 62
9.1.1 Variability in T-bases 62
9.1.1.1 Variability in Ultimate Moment Capacities 62
9.1.1.2 Variability in Material Properties and Geometry 62
9.1.2 Critical Load Orientation 62
9.1.3 Finite Element Model Validation 63
9.1.4 Parametric Study of Key Dimensional Parameters 63
9.1.4.1 Top Bolt Circle 63
9.1.4.2 Bottom Bolt Circle 64
9.1.4.3 Base Plate Thickness 64
9.1.4.4 Pole Diameter 64
9.1.4.5 Interaction of Key Dimensional Parameters 64
9.1.5 Comparison of 1975 and 1985 AASHTO Standard T-Bases 64

9.1.6 Leveling Devices 65
9.2 Recommendations 65

APPENDICES 67
A Result Tables 68
A.1 Average Tensile Strength of Each T-base 68
A.2 Modulus of Elasticity of Each T-base 70
A.3 Hardness Test Results for Transformer Bases 72
A.4 Summary of Results from Experimental Testing and FEM Analysis 73

B Listing of Computer Program INT.FOR to Find the Moment Capacity of TB1-17 and TB3-17 76

LIST OF TABLES

Table

4.1	Comparison of stresses and deflections for different loading orientations	13
5.1	Physical dimensions of t-bases	20
5.2	Test schedule for transformer bases	21
5.3	Static test results for T-bases (TB1-17)	23
5.4	Static test results for T-bases (TB1-20 and TB3-20)	28
5.5	Static test results for T-bases (TB3-17)	29
5.6	Material properties test results for T-bases	33
5.7	Mechanical properties of T-bases as provided by the manufacturer	33
7.1	FEM parametric study for TB1-17	49
7.2	FEM parametric study for TB3-17	50
7.3	Minimum and maximum parameters used in the study	51
7.4	Comparison of moment capacity for TB1-17 and TB1-20	57
7.5	Comparison of moment capacity for TB3-17 and TB3-20	58

LIST OF FIGURES

Figure		
1.1	Actual T-Base installed in the field	2
4.1	Different possible load orientations	8
4.2	Finite element discretization of t-base and base plate	10
4.3	Enlarged deformation of t-base	12
5.1	Test frame	15
5.2	Laboratory setup of T-base/ light pole	17
5.3	Detailed sketch of plan and elevation of laboratory test setup	18
6.1	Finite element discretization of t-base/light pole system	36
6.2	Enlarged deformation of t-base/light pole system	36
6.3	Comparison of strains in the base plate at gage location 6	39
6.4	Comparison of strains in the base plate at gage location 7	40
6.5	Comparison of strains in the base plate at gage location 9	42
6.6	Comparison of strains in the base plate at gage location 10	43
6.7	Comparison of strains in the base plate at gage location 12	44
6.8	Comparison of strains in the base plate at gage location 13	45
7.1	L/T ratio versus Ultimate Moment	55

1. INTRODUCTION

1.1 Overview

Safety considerations during vehicular impact on steel or concrete poles brought out the concept of breakaway supports (also called breakaway bases) placed in between the poles and their concrete foundations. These poles were used to support sign, luminaire or other traffic signals, and the breakaway bases in addition to supporting the poles are also utilized to house transformers and hence were called transformer bases. In short, these transformer bases were called as t-bases and this name is used throughout this report. In Figure 1.1, one of the actual t-bases installed in the field is shown.

1.2 Functionality of the T-base

The functionality of the t-base can be broadly classified into two categories based on the design considerations.

1. T-bases were designed primarily based on their collapsibility due to an automobile collision, and therefore these t-bases were made out of cast aluminum alloy, a brittle material.
2. In addition, t-bases were required to resist an applied moment caused by lateral loads on the luminaire poles due to wind forces.

Dynamic collision tests were conducted on the t-base/light pole systems in the past to determine the collapsibility of the t-base due to an automobile impact. These tests were reported to be very successful

Since the t-bases have to transfer the moment on the light pole due to lateral wind forces to a circular concrete pier foundation, pole manufacturers were required to certify the ultimate moment capacity of their t-base/light pole system using full scale experiments loaded to failure or to the required ultimate capacity. However, to the knowledge of the author, no one has tried to analyze the stresses in the t-bases as they were subjected to bending moments.

1.3 Problem Statement

In 1990, the Federal Highway Administration adopted the new and stricter 1985 American Association of State Highway and Transportation Officials (AASHTO) light pole t-base breakaway requirements. Following this adoption, new t-bases were developed with reduced heights of 17 inches in lieu of 20 inches. The t-bases which meet the 1985 AASHTO requirements have various overall dimensions and are made to use various bolt circle diameters at top and bottom. In addition, the light poles which are bolted onto the t-bases have also various bolt circle diameters, pole diameters at the base plate with variable base plate dimensions and thickness.

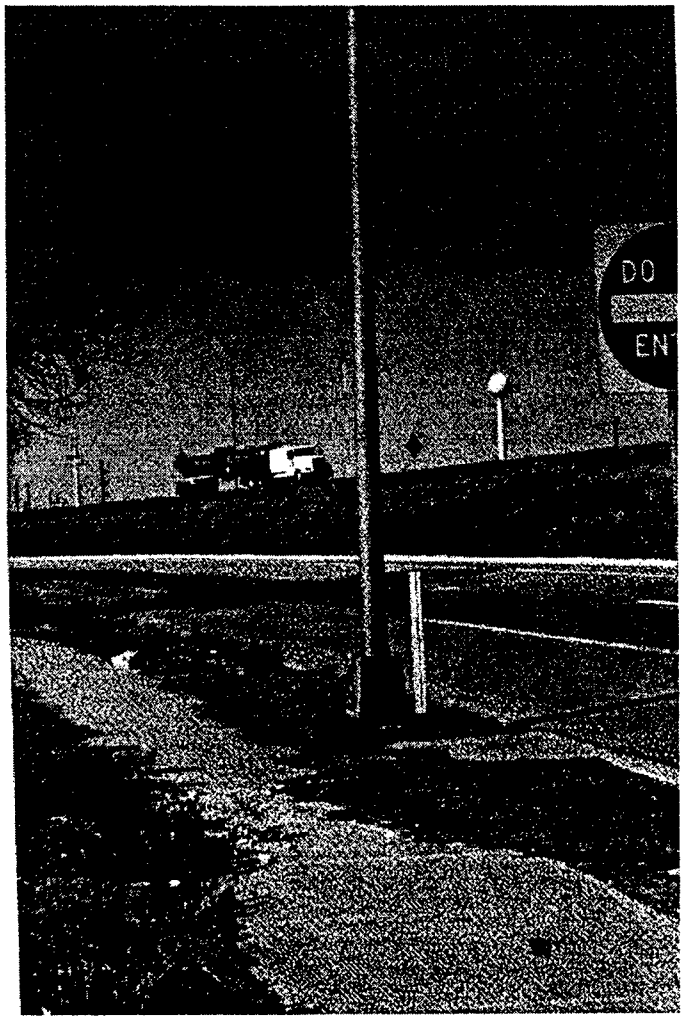

Figure 1.1 Actual T-Base Installed in th eField

Light poles with compatible t-bases have been proven capable of resisting required transverse loads and moments as a single unit. However, concerns have arisen over replacing an existing light pole or t-base with one that has a different dimension(s) or is a different model since the effect of various combinations of the above parameters on the ability of a t-base/light pole system to resist transverse loads has not been clearly defined to date. Current TxDOT policy is to replace with like kind parts. This policy creates an increased logistical problem for the maintenance personnel and increases the cost of maintenance and replacement part inventory.

2. REVIEW OF PAST RESEARCH

A literature review was conducted utilizing the Transportation Information Service (TRIS). Several documents have been identified which reported on the dynamic testing of t-bases where the collapsibility of the base due to an automobile collision was investigated. Since these bases also have to withstand an applied moment due to lateral loads such as wind, TxDOT has been getting these t-bases tested to determine their ultimate moment capacity for the past several years. These tests were full scale tests on t-bases that were bolted to light pole base plates at the top and bolted to concrete test blocks or steel frames at the bottom. Shrestha, et al, (1993) collected most of the available data on these full scale static tests in an effort to correlate the effects of the various parameters that may control the performance of the t-base/light pole system. However, too many parameters were varied between tests, and the tests were conducted in slightly different forms. Their report suggested that no specific conclusions could be drawn without further testing.

Even though a significant amount of static test data were available, it appears that tests have not been coordinated to isolate a specific parameter to evaluate its effect on the strength of the overall system. Predominantly, tests were conducted to verify the strength of a specific t-base/light pole combination. Static tests were performed by mounting the t-base and light pole as described above and applying a transverse load at the end of the test pole, thereby inducing a moment on the t-base. The load was applied until the t-base failed. Moreover, more than one variable was sometimes changed between tests, making it difficult to evaluate the effect of the parameters on the strength of the overall system.

The static test data reported in Shrestha (1993), was reviewed and considered for use in this study. Even though there was a significant amount of static test data reported by Shrestha (1993), several key factors hindered its use in most of this report. A large amount of the data was from tests with the load orientations that were different from the critical orientation determined during this study. The test data reported by Shrestha was review for load orientation effects and it had a general trend which confirmed the results of the finite element analyses conducted during the critical load orientation portion of this study which are presented in Chapter 4. In addition, several tests reported results of exactly the same value which is highly improbable for these types of test. It was also noted that the previously reported ultimate moment capacities for the t-bases were for different locations, some at the top of the t-base while some were at the bottom of the t-base. The t-base test data that were reported by Shrestha was for t-bases which were from many different casting and heat treating lots which was inconsistent with the parametric studies conducted during this project. In addition, the previous test data included many parameter dimensions and t-base models which did not match this study. Therefore, the majority of the previously reported test data was not used in the study but was used for initial understanding and guidance in the development of the current study.

3. RESEARCH APPROACH

The objective of this research was to determine the strength of the t-bases as they are subjected to lateral forces such as wind loads. This strength is measured in terms of its ability to withstand bending moments at the top of the t-base. From a strength of materials point of view, the ultimate moment capacity of this brittle aluminum casting depends on the stress concentrations induced during loading. Stress concentrations are induced by the pull of the bolts in their respective slots. The side opening in the t-base also provides ample scope for some stress concentrations within the overall t-base body. A review of the literature and discussions with Karl Burkett, Traffic Operations Division, TxDOT, indicate that failures commonly initiate at the top or bottom tension corner of the t-base where stress concentrations occur as the load is transferred from the light pole to the t-base via the bolts, or from the t-base to the foundation. The following are the important factors the control the strength of a t-base:

3.1 Variability in the Material

T-bases were made of cast aluminum. The material properties of the t-bases were dictated by its non-homogeneity which can happen from the variation of the material properties and fabrication techniques such as casting, welding, heat treating and so on. To understand the effects of the material variability, the t-bases were purchased from different sources at different times. The various purchases and their sources are recorded in Chapter 5 of this report. In addition, test coupons were cut from the t-bases after ultimate moment testing. They were subjected to uniaxial tension tests where the values of modulus of elasticity and ultimate strength were determined. At least three test coupons were cut from each t-base. The results are tabulated in Appendix A.1 and A.2. Besides these tests, the test coupons were also tested for material hardness using Rockwell Hardness Testing Machine. The results obtained form these tests are also documented in Appendix A.3.

3.2 Critical Load Orientation on the T-base.

Because of the presence of the door on the side of the t-base, there are five axes where the strength of the t-base can determined. These different cases are discussed in the next chapter. The critical or the weakest orientation of the t-base has to be investigated. This study is done by using the finite element model.

3.3 Controlling Parameters or Dimensions During Fixing a T-Base.

The t-base was designed with special slots to allow variable bolt circles to be used at the top and bottom of the base. According to field engineers involved with these systems, a reduction in the size of the bolt circle diameter could be detrimental to the load carrying capacity of the t-base. There are many parameters that controlled the overall behavior of the system and the primary ones are listed below.

1. Bolt circle diameter at the top, d_t
2. Bolt circle diameter at the bottom, d_b

3. Thickness of the base plate, t
4. Diameter of the light Pole, d_P

The magnitude of the ultimate moment capacity of the t-base system varies with the size of the bolt circle diameters, thickness of base plates and pole diameters that are commonly used in the field. To investigate this, detailed experiments are performed in the laboratory. The experiments conducted on different t-bases indicated that even by keeping all the parameters constant the resulting moment capacity of each t-base varied significantly.

The finite element model being a numerical model, was used to investigate the effect of the parameters, while keeping the material properties constant. The model will allow weak regions in the t-base to be located and studied very effectively. A technique was developed to determine a lower bound ultimate moment capacity of a t-base with specified magnitudes of the controlling parameters using the finite element model and the results were compared with those obtained from the experiments. Now that the technique has been developed and verified, similar techniques can be used in the future for further studies as funding allows.

3.4 A Simple Computer Code for Strength of a T-Base System.

For the convenience of engineers using t-bases in the field with different controlling parameters, a simple interpolation technique was employed that would give an estimate of the ultimate capacity of a t-base for the parameters that are used in the field.

3.5 Recommendations and Guidelines.

This report also provides guide lines and recommendations based on the parametric study conducted using elaborate experiments and finite element analysis. Suggestions for improvements or modifications to be incorporated in the overall design of the t-base in order to further increase the performance of the system are also made at the end of this report.

4. CRITICAL LOAD ORIENTATION

4.1 Introduction

Different load orientations were possible due to the presence of a side opening or what is called 'door'. Once the critical load orientation was established, static tests and Finite Element Analysis were planned to be conducted only in the critical loading direction. Using finite element analyses, the behavior of a t-base for all the possible load orientations was studied and the critical load orientation was established. These details are given in the following sections, and Figure 4.1 shows these possible load orientations. Determination of critical load orientation forms a major task of this research.

4.2 Loading Orientations

Part of the complication associated with the scrutiny of the results of the previously published test data also depended on the presence of the existing door on one side of the t-base. In the past, this door was used for convenience for the placement of the transformer equipment; however, now it is used for tightening the anchor bolts to the foundation and the placement of the bolts connecting the pole base plate to the t-base. Even if one assumes that all the other parameters are symmetric with respect to four vertical planes, the side door in the t-base creates a lack of symmetry; In other words, the t-base is symmetric only with respect to a vertical plane passing through the center of the door. This creates five distinct loading orientations that are critical to the overall behavior and ultimate strength of the t-base/light pole system. The testing agencies have formerly identified these orientations with two general cases.

1. The moment applied about an axis parallel to a diagonal of the t-base.
2. The moment applied about an axis parallel to the side of the t-base.

These two general cases lead to five distinct load cases, while the first general case results in two distinct cases and the second general case results in three distinct cases. These five distinct load cases are described below.

For the first general case, where the moment is applied about an axis parallel to the diagonal, we have;

1. Door on the tension side, Door in Diagonal Tension (DDT).
2. Door on the compression side, Door in Diagonal Compression (DDC).

For the second general case, when the moment is applied about an axis parallel to the side of t-base, we have;

3. Door located on the neutral axis, Door on Neutral Axis (DNA).
4. Door located on the compression side, Door in Compression (DIC).
5. Door located on the tension side, Door in Tension (DIT).

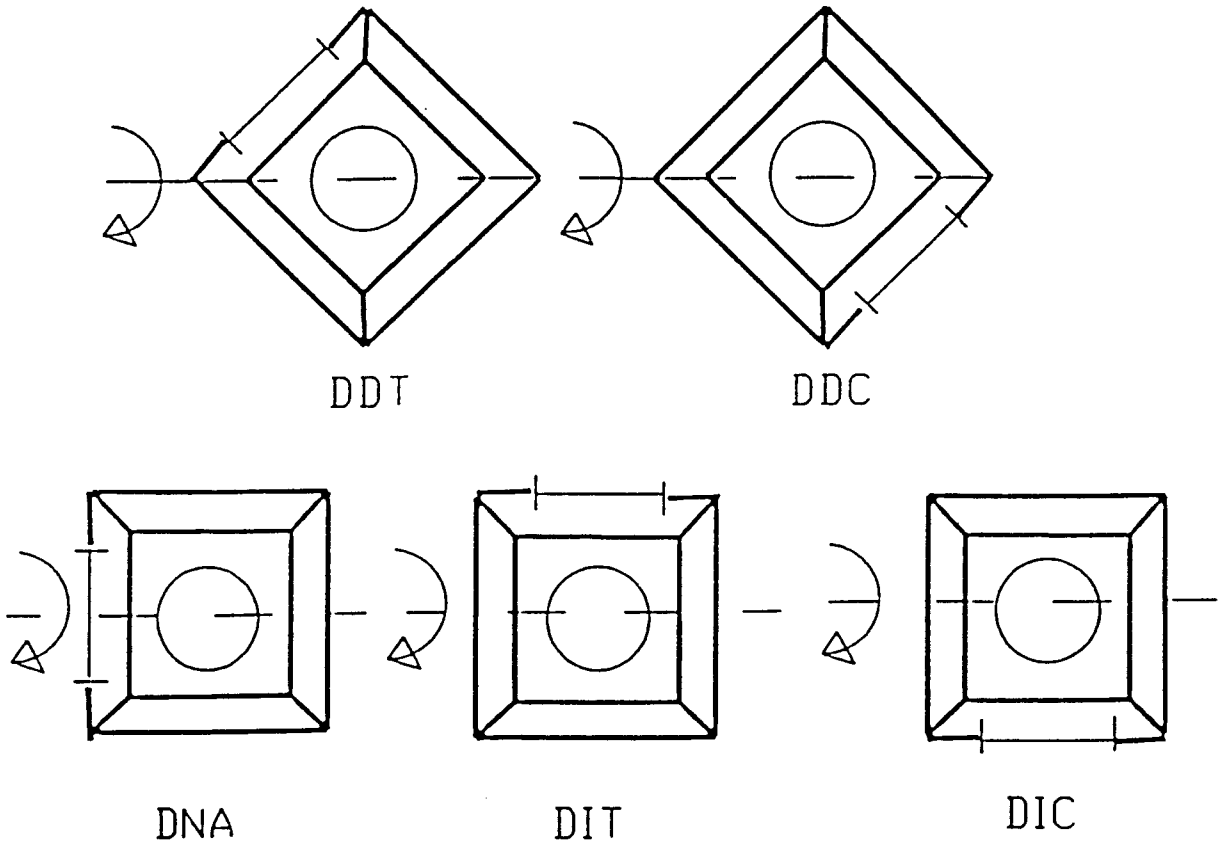

Fig. 4.1 Different Possible Load Orientations

4.3 Finite Element Modeling

Finite element method is a well proven technique and is being used to solve the most complex problems in solid mechanics. A numerical finite element model was developed to study the effect of the five load orientations. There are many general purpose finite element softwares available for structural analysis. CSA/NASTRAN, a versatile finite element code was selected for this purpose. CSA/NASTRAN is only an analytical tool and it needs a pre-processor for modeling the structure and a post-processor for processing the results. A powerful pre and post processor FEMAP with advanced modeling features has been utilized for this purpose.

Two types of elements were employed in this modeling. In the first model, a plate and shell element was used to model the t-base/pole base plate. Because the load was transferred from the pole base plate to the t-base through bolts, the shell finite elements were found to be inadequate for accurate modeling. Moreover, the internal ribs that are provided to strengthen the connection between the vertical walls and the horizontal flange portions of the t-base could not be properly modeled. The second approach was to use eight noded and six noded, three dimensional solid brick elements to model the t-base, base plate, and bolts. Though complicated, the stiffening ribs were included in the model.

The pole base plate is connected to the t-base by bolts, and this connection creates a very complex interaction between the base plate and the top of the t-base. We assumed that there is no initial tension in the bolts and that when a gap developed between the two contacting surfaces, then the vertical contact stress between the base plate and the top of the t-base will be zero. In other words, the base plate looses the contact with top of the t-base there by creating a physical gap between two surfaces. On the other hand, the regions where contact between the two surfaces occurs, vertical compressive stresses are developed. The interaction between the t-base and the base plate was modeled by employing gap elements between the two surfaces. Also to simulate the actual load transfer from the pole to the t-base, gap elements were provided between the contact surfaces of the bolts, t-base, and base plate. A similar set up with gap elements was used to model the connections between the t-base and the anchor bolts in the pier foundation with the bottom of the anchor bolts assumed to have zero displacements.

Figures 4.2a, 4.2b, 4.2c and 4.2d indicate the finite element discretization of a TB1-17 t-base with a *32mm.(1.25 in)* thick base plate having a circular hole *203.2 mm.(8 in)* in diameter. There are 6,984 solid elements with a total of 30,390 degrees of freedom for the model. The number of gap elements are 792. The thickness of the t-base shell was taken as 0.25 in. except at places where the thickness could not be measured accurately. Because of the required matching between the top of the t-base and the base plate at the gap element locations, the circular bolts and their bolt heads could not be modeled perfectly circular. However, every effort is made to keep the overall cross sectional area of the bolts and the bolt heads approximately the same as the perfectly circular bolts and bolt heads. Even though only linear material properties are used in this analysis, the use of gap elements required several iterations in order to arrive at the final solution. One complete solution took almost 3.0 hours on a PC with 60MHz processing speed. The

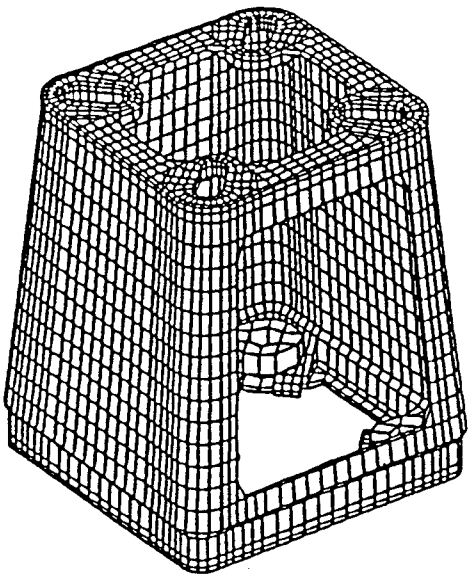

(a) View from Top

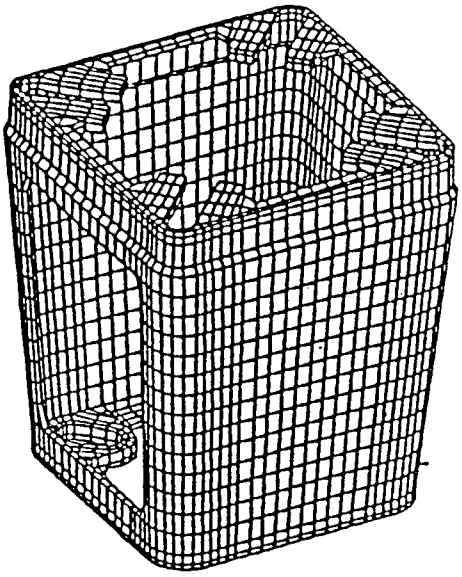

(b) View from Bottom

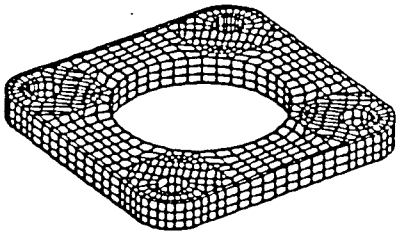

(c) Base Plate

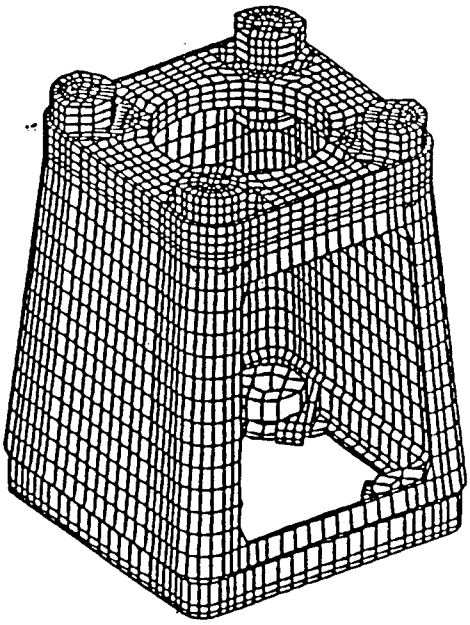

(d) Combined Model

Figure 4.2 Finite Element Discretization of T-base and Base Plate

finite element model was subjected to a moment equal to 10,000 ft-lb. Figure 4.3 illustrates the enlarged deformation in the t-base, when the moment is applied with its axis on the diagonal of the t-base. It is interesting to observe the deformation pattern of the top of t-base and base plate due to the complex interaction occurring between them and the anchor bolts. The loading orientation corresponds to DDT, i.e. door in diagonal tension. In this analysis, it was assumed that the bolts have no initial tension.

4.4 Comparison of Stresses and Displacements in Different Loading Orientations

One of the problems faced when evaluating the ultimate moment capacity of the t-bases was to establish the critical load orientation which results in its worst behavior. Even though many static tests have been conducted, variations of the parameters and material non-homogeneity did not allow any definite conclusions to be reached with regard to the critical load orientation. However, a review of the previous test data did indicate a general trend toward DDT being the critical load orientation. To overcome this dilemma, an example problem was selected and finite element analyses were conducted while all the parameters were held constant with the exception of the loading orientations. A comparison of the results for maximum displacements and maximum stresses in the base plate and t-base for the five different orientations is shown in Table 4.1. These results correspond to an applied moment of 10,000 ft-lb. as mentioned earlier. A discussion on these results is given in the next section.

4.5 Discussion of Results

In Table 4.1, results are presented for maximum vertical deflection of the structure and maximum principal stresses in the base plate and the t-base. The location of these stresses is also given. The maximum displacements were occurring in the base plate for the case of DIT and the next for DDT. Also, the maximum stress was observed in the base plate for the case of DIT, but the maximum stress in the t-base was occurring for the case of DDT. It should be recognized that maximum stresses in the t-base are critical and will control failure. The results indicate that the maximum stress in the t-base corresponds to DDT with a magnitude of 15,745 psi which is significantly higher than the other four load orientations. Hence, it can be concluded that the orientation with moment applied about the diagonal direction with the door in tension (DDT, door in diagonal tension) was found to be the critical load orientation for determining the ultimate moment capacity of the t-base. These stresses and deflections will vary depending on the base plate thickness, bolt circle diameters and pole diameter, etc.

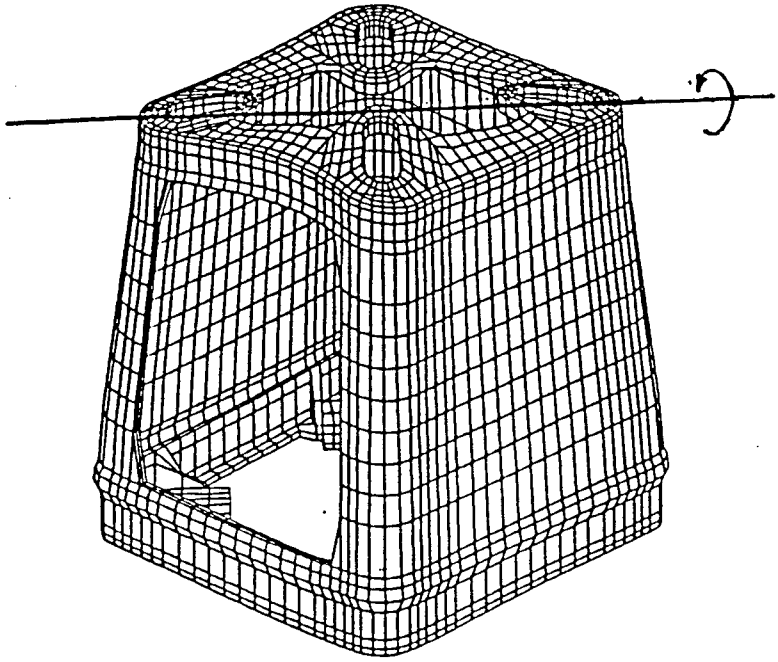

Fig. 4.3 Enlarged Deformation of T-base

Table 4.1. Comparison of Stresses and Deflections for Different Loading Orientations

Case		DDT	DDC	DNA	DIT	DIC
Base Plate	Maximum Vertical Deflection (inch)	0.018	0.014	0.017	0.023	0.016
T-Base	Maximum Stress (psi)	15,745	11,197	10,842	11,426	9,662
T-Base	Location	Tension side near bottom rib	Tension side near bottom rib	Tension side near bottom rib	Tension side near bottom rib	Tension side near bottom rib

Note: 1 inch = 25.4 mm
1 psi = 6.895 kPa

5. EXPERIMENTAL SETUP AND PARAMETRIC STUDY

5.1 Experimental Procedure to Determine the Structural Strength of T-Base

5.1.1 Introduction

The objective of this experimental setup was to study the effects of the parameters mentioned in the previous chapter that influence the moment capacity of the t-base. In field applications, the light pole/t-base system is vertical and the system is subjected to lateral wind forces which creates moments in the t-base. In the field, the light pole /t-base system is bolted onto a concrete pier foundation buried in the soil. For convenience during laboratory testing, the whole t-base/light pole system was installed horizontally. The lateral force was applied in a horizontal plane and the axis of the moment was kept vertical instead of horizontal as in field situations. Also, the load was applied as a concentrated force at one end of the pole. As mentioned earlier, the loading orientation, DDT (door in diagonal tension) was found to be critical from the finite element analysis, and so in this experimental study, all the t-bases were tested keeping the door in diagonal tension.

A cable from a loading winch was employed to pull the end of the pole, thereby producing a concentrated force at the end of the pole. The load was applied gradually until failure of the t-base occurred. A pre-calibrated load bar using strain gages was used to measure the force in the cable. Strain gages were also mounted on both sides of the pole close to the base plate to determine the induced moment on the t-base top. A computer based data acquisition system was used to collect the readings from all the strain gages. The following sections describe the whole experimental setup and procedure in detail.

5.1.2 Test Frame Representing Concrete Pier Foundation

To simulate the concrete pier foundation in the laboratory, a steel test frame was specially fabricated for this experiment using 413.7 Mpa (60 ksi) (yield strength) steel plates. The test frame was L-shaped with ribs connecting the two arms of the frame on both sides. One arm of the test frame was bolted firmly onto the concrete floor of the laboratory using four 31.75mm (1.25 in) diameter threaded rods. On the other arm of the test frame which was vertical, four slots of 146.05 mm (5.75 in) long and 33.53 mm (1.32 in) wide were made. The slots were arranged in such a way that they could allow different bottom bolt circle diameter of t-base which was one of the test parameters to be investigated. The center of the square slot-zone was 508 mm (20 in) from the laboratory floor and the centroidal longitudinal axis of the t-base/light pole system coincided with slot-zone center. The test frame is shown in Figure 5.1.

5.1.3 T-base/Light Pole Setup

In this experiment, the system consisted of three parts. First, the t-base was bolted to the test frame. Second, a 0.914 m (3 ft) section of pipe with base plates welded at both ends was connected to the base plate of a 6.1 m (20 ft) long 203.2 mm (8 in) pipe.

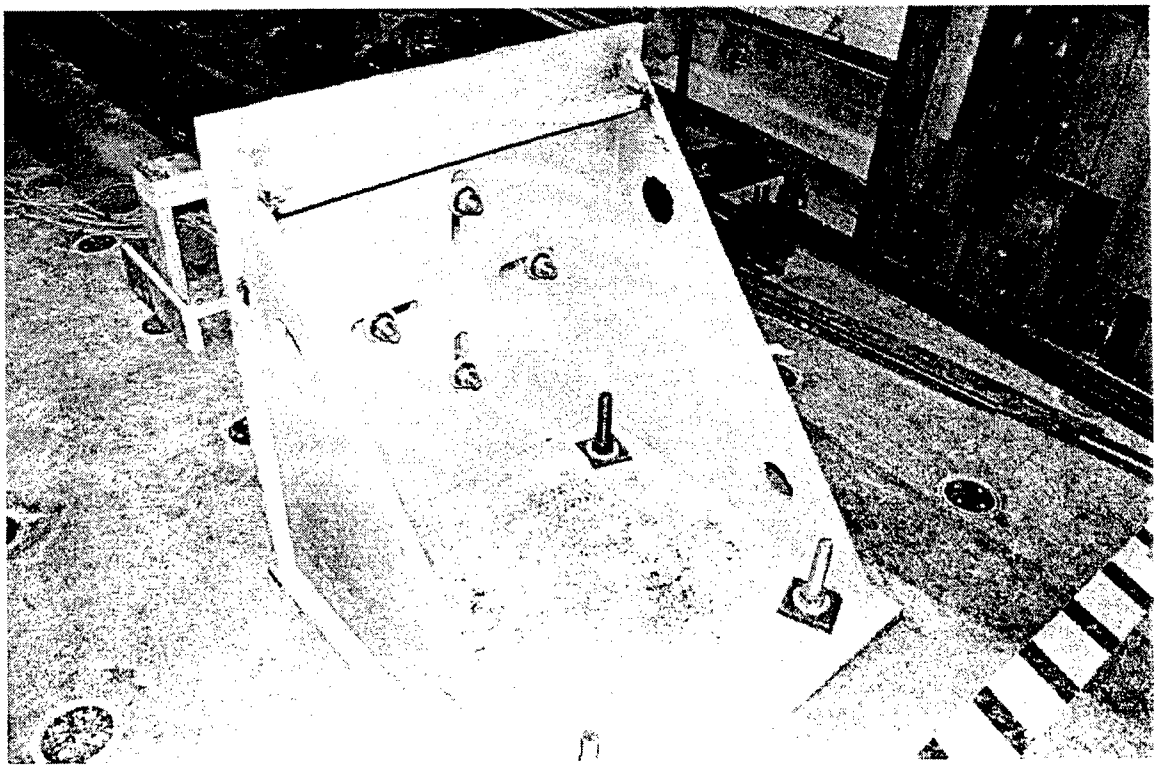

Fig. 5.1 Test Frame

Finally, the t-base top was bolted to the other base plate of the three foot section pipe. The reason for using the three foot section pipes instead of a continuous pipe was to avoid changing the test pole by rewelding a new base plate at its bottom for each test. The connection between the 0.914 m (3 ft) section pipe and the main pipe was made using steel base plates and bolts. Three separate assemblies of 0.914 m (3 ft) section pipes and plates were prefabricated with required base plate size, thickness, and top bolt circle diameter according to the test plan. Figure 5.2 shows the laboratory t-base/light pole setup.

A roller support, on which the pole rested, was used 5.79 m (19 ft) away from the top of the t-base on which the pole rested. This roller support allowed free movement of the end of the t-base/light pole system during the loading operation and minimized any friction between the support and the laboratory floor. The support was necessary to avoid moments induced about a horizontal axis at the top of the t-base due to the self weight of the pole. The t-base and light pole system was aligned in such a way that the centroidal longitudinal axis of the pole and the load winch and the cable were in the same horizontal plane 508 mm (20 in) above the laboratory floor. A detailed plan and elevation of the laboratory setup is shown in figure 5.3.

5.1.4 Load Bar Calibration

Since the loading winch did not have any mechanism to indicate the force applied during loading operation, a precalibrated load bar was used along with the loading cable to determine the applied force on the pole. The measured force on the pole was then multiplied by the distance from the loading point to the top of the t-base to obtain the applied moment on the t-base. The load bar used was 279.4 mm (11 in) long, 50.8 mm (2 in) wide and 6.35 mm (0.25 in) thick and was made of A36 steel.

The load bar was calibrated with strain gages mounted on the center of both sides of the bar. A tensile load was applied to the bar by a universal testing machine and signals from the gages were collected with the data acquisition system. The tensile load on the bar was varied from 0 N (0 lb) to 13,344 N (3,000 lb). At each load interval, the voltage signals from strain gages were collected in the computer and later processed into strains using the strain conversion equation discussed earlier in the chapter. The bar calibration was done three times using three different load intervals, and the average values of strains from these three runs were then used to establish a load-strain chart.

5.1.5 Key Dimensional Parametric Study

The moment capacity of a t-base depends on four key dimensional parameters. These parameters are:

1. Top bolt circle diameter (d_t),
2. Bottom bolt circle diameter (d_b),
3. Base plate thickness (t), and
4. Diameter of the pole at the base plate level (d_p).

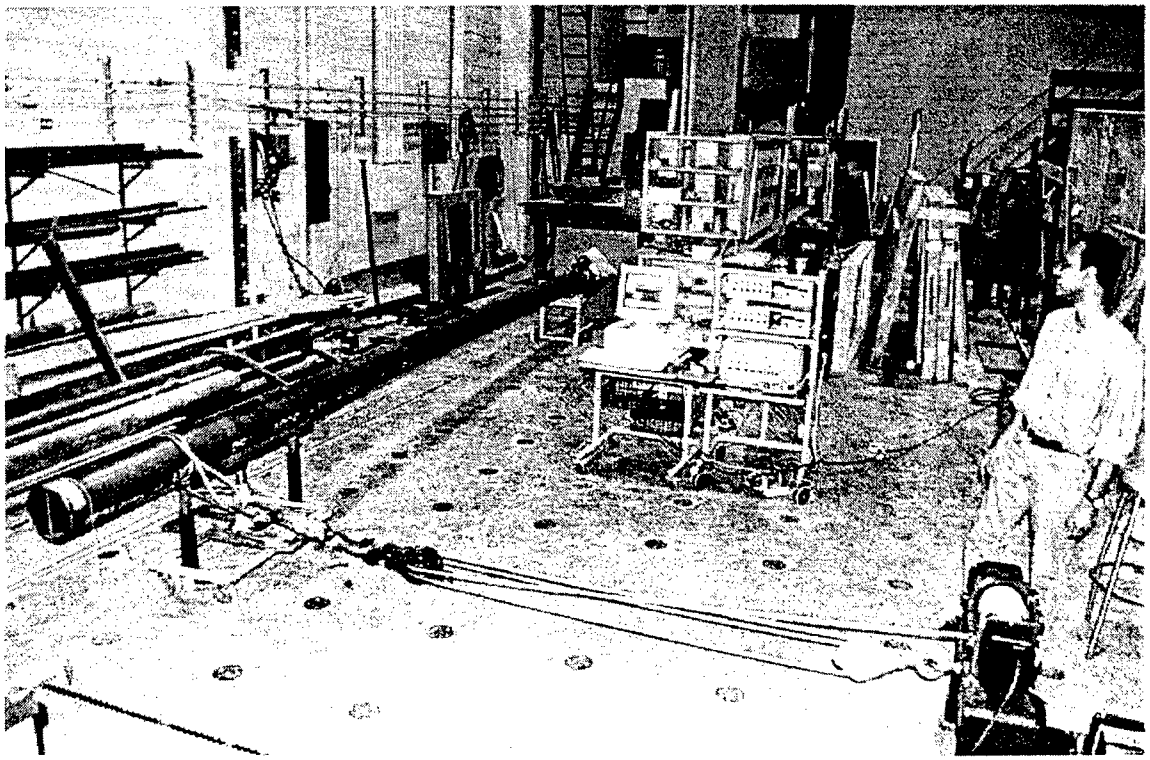

Fig. 5.2 Laboratory T-Base/ Light Pole Setup

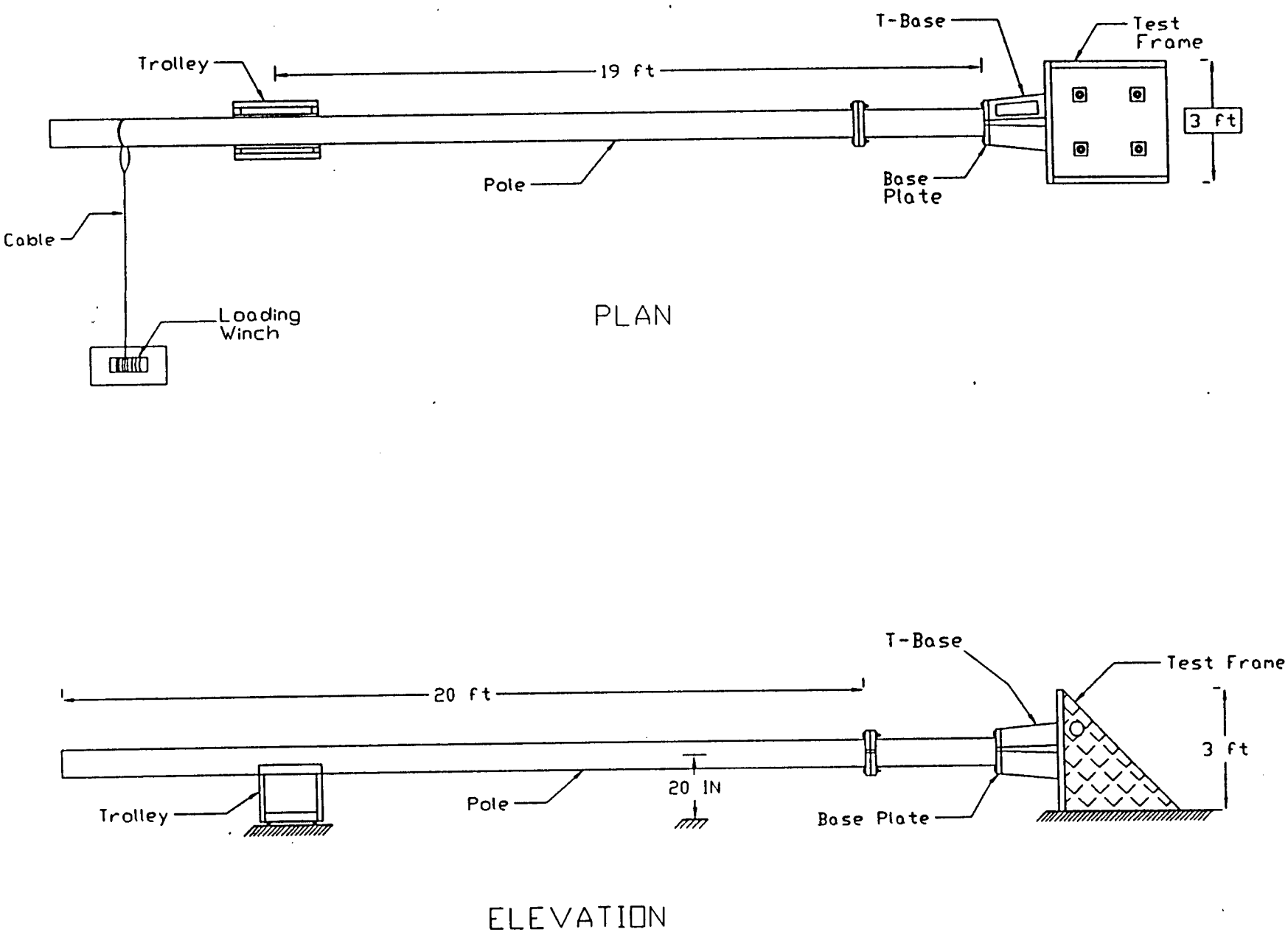

Fig. 5.3 Detailed sketch of plan and elevation of laboratory setup

In the parametric study, the effects of all these parameters on the moment capacities of t-bases were investigated separately and in combination. The values of the parameters which were investigated for the TB1-17 were; top bolt circle diameters 279.4 and 342.9 mm (11 and 13.5 inches), bottom bolt circle diameters of 330.2 and 381 mm (13 and 15 inches), base plate thicknesses 25 mm (1 in) and 32 mm (1.25 in) and pole diameters of 177.8 and 203.2 mm (7 and 8 inches). The investigated parameter values for the TB3-17 were; top bolt circle diameter 381 mm (15 in), bottom bolt circle diameters 381 and 431.8 mm (15 and 17 inches), base plate thickness 32 and 38 mm (1.25 and 1.5 inches), and pole diameter 241.3 mm (9.5 in) were investigated.

5.1.6 Test Plan

A test plan was developed prior to testing, incorporating the key dimensional parameters and other factors that might affect the test program. Four different models of t-bases were purchased from three different distributors in seven different lots using the seven purchase orders shown in Table 5.1. Identical models of t-bases (both TB1-17 and TB3-17) were purchased from different suppliers or at different times and tested with similar dimensional parameters to study the variability of the t-base's strength caused by different casting and heat treating lots. The t-bases used in the quality control study are identified by model number and purchase order number in Table 5.2. Adequate quantities of both TB1-17's and TB3-17's were purchased from a single supplier at one time for use in the parametric study of each model, identified in Table 5.2. T-bases of both 1975 standard (TB1-20 and TB3-20) and 1985 standard (TB1-17 and TB3-17) were included in these t-base lots and moment capacities of these two standards were also determined and compared. Table 5.1 show the physical dimensions of the t-bases purchased, obtained from the manufacture or the distributor. Table 5.2 shows the test schedule for this research project and indicates the purpose of each test. Three different pole diameters, two different base plate thickness, four different top bolt circle diameters and three different bottom bolt circle diameters were investigated. To determine the moment capacities of t-bases, AASHTO requires three t-bases be broken and the average breaking moment be calculated. If each of the breaking moments is within 10% of the average breaking moment, then the average breaking moment is taken as the moment capacity of the breakaway t-bases. Following AASHTO requirement, for a particular set of parameters, three tests were performed. Sometimes more than three tests were performed for the same set of parameters to get the breaking moment of the t-bases of that group within 10% of the average breaking moment of that group. When the breaking moment of any one t-base was not within 10% of the average breaking moment of the 3 t-bases, one or more t-bases were tested until at least 3 t-bases broke within 10% of their average value. This average value was then used as the breaking moment for the series of tests. It was decided that any 3 test values falling within 10% of their average value was statistically significant and therefore satisfactory.

5.1.7 Test Procedure

The procedure outlined here was common to all t-base specimens. First of all, the t-base was bolted to the test frame with the required bottom bolt circle diameter. Then the

Table 5.1. Physical Dimensions of T-bases.

T-base Designation	Distributor	Purchase Order NO.	T-base Height, H (in.)	Bolt Circle Diameter	
				Top min.-max. (in.)	Bottom min.-max. (in.)
TB1-17	A-1 Industrial Supply, Hayward, CA.	615643	17	10.5-13.5	13.0-15.0
TB1-17	A-1 Industrial Supply, Hayward, CA.	616576	17	10.5-13.5	13.0-15.0
TB1-17	John Knole Industries, Lubbock, TX.	616544	17	10.5-13.5	13.0-15.0
TB1-17	JEM Engineering and Manufacturing Co., Inc., Tulsa, OK.	616582	17	10.5-13.5	13.0-15.0
TB3-17	A-1 Industrial Supply, Hayward, CA.	615643	17	13.0-15.125	15.0-17.25
TB3-17	A-1 Industrial Supply, Hayward, CA.	61601	17	13.0-15.125	15.0-17.25
TB1-20	A-1 Industrial Supply, Hayward, CA.	616557	20	11.0-13.0	13.0-15.0
TB3-20	A-1 Industrial Supply, Hayward, CA.	612280	20	13.0-15.125	15.0-17.25

Note : All the transformer bases were manufactured by the Akron Foundry Company, Akron, Ohio.

Table 5.2. Test Schedule for Transformer Bases.

P.O. No.	T-base ID	Pole Dia d_p (in.)	Base Plate Thk t (in.)	Top Bolt Circle d_t (in.)	Bottom Bolt Circle d_b (in.)	Remarks
616576	TB1-17	8	1.25	13.5	15	See Note 1,2 and 3
616576	TB1-17	8	1.25	11	15	See Note 1
616576	TB1-17	8	1	13.5	15	See Note 1
616576	TB1-17	8	1	11	15	See Note 1
616576	TB1-17	7	1.25	13.5	15	See Note 1
616576	TB1-17	7	1.25	11	15	See Note 1
616576	TB1-17	8	1.25	13.5	13	See Note 1
616576	TB1-17	7	1.25	13.5	13	See Note 1
616582	TB1-17	8	1.25	13.5	15	See Note 2
616544	TB1-17	8	1.25	13.5	15	See Note 2
615643	TB1-17	8	1.25	13.25	15	See Note 4
616557	TB1-20	8	1.25	13.5	15	See Note 3
615643	TB3-17	9.5	1.25	15	17	See Note 2 and 3
616601	TB3-17	9.5	1.25	15	17	See Note 1,2 and 3
616601	TB3-17	9.5	1.25	15	15	See Note 1
616601	TB3-17	9.5	1.5	15	17	See Note 1
612280	TB3-20	9.5	1.25	15	17	See Note 3

Notes :

1. Parametric study.
2. Quality control study.
3. Strength study of 1975 and 1985 AASHTO standards.
4. Washer influence study.
5. 1 inch = 25.4 mm

0.914 m (3 ft) section test pole with base plates welded on its both ends was bolted to the 6.1 m (20 ft) long pipe base plate. The other end of the three feet section was then bolted onto the top of the t-base using the required top bolt circle diameter and base plate thickness. The 6.1 m (20 ft) pipe was supported by the roller support mentioned earlier 5.79 m (19 ft) away from the top of t-base. A loading winch of 35,584 N (8000 lb) capacity, was placed 3.05 m (10 ft). away from the pipe in a direction perpendicular to the pipe. The load bar was connected to the cable of the winch at one end and to the pipe at the other end. The cable was passed through a two pulley-system to control the rate of loading. The loading winch and the load bar were placed 6.4 m (21 ft) away from the t-base top. All the strain gages mounted on the load bar and pole were connected to the signal conditioner and amplifier with wires. The outputs from the amplifiers were linked to the EXP-16 multiplexer board which was in turn hooked up with the DAS08 inside the

computer. When the connections between the strain gages, amplifier and the computer were made, the amplifier was balanced for each gage. The gain and excitation for each amplifier channel were adjusted for the required range of output voltage.

After the setup was ready, an initial load causing a deflection of 200-250mm (8-10 in) was applied to the t-base/light pole system to take out any slack in the connections. The system was unloaded and all the bolts were retightened using 203.4 N-m (150 ft-lb) of torque. Finally after checking the settings and balancing the data acquisition system, the t-base/light pole system was loaded until the failure of t-base with simultaneous recording of the signals from all the strain gages.

5.2 EXPERIMENTAL RESULTS

5.2.1 Experimental Results

Moment capacities for the t-bases were calculated using strain data from the strain gages located at the pole bottom. Readings from two strain gages installed diagonally opposite on the extreme bending fibers on the pole were averaged to calculate the moments. The absolute values of the strain gage readings were taken to obtain the average because the two readings were approximately equal and opposite (one was under tension and the other was under compression). Breaking moments for the t-bases were also calculated using the load bar and its calibration chart. However, the moments computed using load bar were 10 to 15% higher than those calculated using strain gage readings from the pole. The moments obtained from load bar were discarded and have not been reported herein. There were two reasons for discarding the load bar moments; the roller support which was used near the loading end of the pole induced some frictional resistance which in turn caused higher load bar forces and calculated moments, and the position of the load bar (wide face horizontal, vertical or inclined) during loading operation might have created some unexpected bending or twisting strain that couldn't be separated from pure tensile strain.

Test 1 using TB1-17 sample was conducted as a pilot test and was loaded only to the elastic limit. This test was repeated several times and experimental strain readings at different strategic locations of the t-base and base plate were obtained for comparison to strains obtained from finite element analysis. This sample was not broken. Table 5.3, Table 5.4 and Table 5.5 list all the breaking moments for TB1-17, TB1-20 and TB3-20, and TB3-17, respectively.

5.2.2 T-base Failure Location

The failure location of each t-base tested is provided in Tables 5.3, 5.4, and 5.5. All but one of the observed failures were tensile fractures which occurred near the top or bottom of the t-base. Thirty-one tensile fractures occurred at the top of the t-base at the juncture of its side wall and top flange. Twenty-seven tensile fractures occurred near the bottom of the t-base either at the juncture of the side-wall and bottom flange or at the welded joining the top and bottom pieces of the t-base which are cast separately and then welded together. The location of the tensile fractures varied randomly, even between tests

Table 5.3. Static Test Results for T-bases (TB1-17).

Test ID	Test Date	P.O. No.	Pole Dia., d_p (in.)	Square Base Plate Size		T.B.C. d_t (in.)	B.B.C. d_b (in.)	Breaking Moment (ft.-lb.)	Ultimate Moment Avg. of Three (ft.-lb.)	Location of Failure
				Width (in.)	Thk. (in.)					
TB1-17-1		615643	8	13.125	1.25	13.25	15	Not Broken	Was used to Compare Experimental Strain Readings to FEM model Strain Readings	
TB1-17-2	08/01/96		8	13.125	1.25	13.25	15	28,188[a]		Bottom tension corner
TB1-17-3	08/09/96		8	13.125	1.25	13.25	15	33,806[a]	31,557	Bottom tension corner
TB1-17-4	08/21/96		8	13.125	1.25	13.25	15	32,679[a]		Bottom tension corner
TB1-17-5	10/15/96		8	13.125	1.25	13.5	15	43,359[b]		Top tension corner

Note : 1 inch = 25.4 millimeters 1 ft-lb = 1.356 N-m.

[a] Test 2 to Test 4 were done with washers (O.D.= 2.75 in., Thk.=0.5 in.) in between T-base bottom and test frame at four corners of the T-base.

[b] Test 5 was done without any washer in between T-base bottom and test frame to check the difference in breaking moment.

Table 5.3. (Continued)

Test ID	Test Date	P.O. No.	Pole Dia., d_p (in.)	Square Base Plate Size		T.B.C. d_t (in.)	B.B.C. d_b (in.)	Breaking Moment (ft.-lb.)	Ultimate Moment Avg. of Three (ft.-lb.)	Location of Failure
				Width (in.)	Thk. (in.)					
TB1-17-6	10/22/96	616576	8	13.125	1.25	13.5	15	46,230		Bottom tension corner
TB1-17-7	10/22/96	616576	8	13.125	1.25	13.5	15	43,131	44,207	Bottom tension corner
TB1-17-8	10/23/96	616576	8	13.125	1.25	13.5	15	34,960[c]		Bottom tension corner
TB1-17-9	10/23/96	616576	8	13.125	1.25	13.5	15	43,260		Bottom tension corner
TB1-17-10	10/24/96	616582	8	13.125	1.25	13.5	15	37,610		Bottom tension corner
TB1-17-11	10/25/96	616582	8	13.125	1.25	13.5	15	36,440	37,945	Bottom tension corner
TB1-17-12	10/29/96	616582	8	13.125	1.25	13.5	15	39,785		Bottom tension corner

[c] Breaking moment from this test was not within 10% of the average of tests with the same test parameters.

Table 5.3. (Continued)

Test ID	Test Date	P.O. No.	Pole Dia., d_p (in.)	Square Base Plate Size		T.B.C. d_t (in.)	B.B.C. d_b (in.)	Breaking Moment (ft.-lb.)	Ultimate Moment Avg. of Three (ft.-lb.)	Location of Failure
				Width (in.)	Thk. (in.)					
TB1-17-13	10/29/96	616544	8	13.125	1.25	13.5	15.0	48,649		Top tension corner
TB1-17-14	10/29/96	616544	8	13.125	1.25	13.5	15.0	43,488	44,214[d]	Top tension corner
TB1-17-15	10/30/96	616544	8	13.125	1.25	13.5	15.0	44,410		Top tension corner
TB1-17-16	11/08/96	616544	8	13.125	1.25	13.5	15.0	40,308		Bottom tension corner
TB1-17-17	11/08/96	616576	8	13.125	1.25	11.0	15.0	31,793		Top tension corner
TB1-17-18	11/12/96	616576	8	13.125	1.25	11.0	15.0	30,739		Top tension corner
TB1-17-19	11/12/96	616576	8	13.125	1.25	11.0	15.0	35,471[e]	30,799	Top tension corner
TB1-17-20	11/12/96	616576	8	13.125	1.25	11.0	15.0	29,864		Top tension corner

[c] Breaking moment from this test was not within 10% of the average of tests with same test parameters.
[d] Four tests were used to calculate the ultimate moment.

Table 5.3. (Continued)

Test ID	Test Date	P.O. No.	Pole Dia., d_p (in.)	Square Base Plate Size		T.B.C. d_t (in.)	B.B.C. d_b (in.)	Breaking Moment (ft.-lb.)	Ultimate Moment Avg. of Three (ft.-lb.)	Location of Failure
				Width (in.)	Thk. (in.)					
TB1-17-21	11/15/96	616576	8	13.125	1.00	13.5	15.0	38,200		Top tension corner
TB1-17-22	11/21/96	616576	8	13.125	1.00	13.5	15.0	39,138	39,669	Top tension corner
TB1-17-23	12/06/96	616576	8	13.125	1.00	13.5	15.0	41,669		Top tension corner
TB1-17-24	12/16/96	616576	7	13.125	1.25	13.5	15.0	45,027		Top tension corner
TB1-17-25	12/16/96	616576	7	13.125	1.25	13.5	15.0	44,525	44,639	Bottom tension corner
TB1-17-26	12/18/96	616576	7	13.125	1.25	13.5	15.0	44,366		Top tension corner
TB1-17-27	12/18/96	616576	7	13.125	1.25	11.0	15.0	32,409		Top tension corner
TB1-17-28	12/18/96	616576	7	13.125	1.25	11.0	15.0	30,478	30,944	Top tension corner
TB1-17-29	12/19/96	616576	7	13.125	1.25	11.0	15.0	29,946		Top tension corner

Note : 1 inch = 25.4 millimeters 1 ft-lb = 1.356 N-m.

Table 5.3. (Continued)

Test ID	Test Date	P. O. No.	Pole Dia., d_p (in.)	Square Base Plate Size		T.B.C. d_t (in.)	B.B.C. d_b (in.)	Breaking Moment (ft.-lb.)	Ultimate Moment Avg. of Three (ft.-lb.)	Location of Failure
				Width (in.)	Thk. (in.)					
TB1-17-30	12/19/96	616576	8	13.125	1.00	11.0	15.0	29,945	29,945[e]	Top tension corner
TB1-17-31	12/19/96	616576	7	13.125	1.25	13.5	13.0	37,316		Bottom tension corner
TB1-17-32	12/20/96	616576	7	13.125	1.25	13.5	13.0	31,210[c]	37,971	Bottom tension corner
TB1-17-33	12/21/96	616576	7	13.125	1.25	13.5	13.0	38,776		Bottom tension corner
TB1-17-34	12/21/96	616576	7	13.125	1.25	13.5	13.0	37,820		Bottom tension corner
TB1-17-35	12/21/96	616576	8	13.125	1.25	13.5	13.0	40,873		Bottom tension corner
TB1-17-36	12/22/96	616576	8	13.125	1.25	13.5	13.0	39,931	40,697	Bottom tension corner
TB1-17-37	12/22/96	616576	8	13.125	1.25	13.5	13.0	41,286		Bottom tension corner

Note : 1 inch = 25.4 millimeters 1 ft-lb = 1.356 N-m.

[c] Breaking moment from this test was not within 10% of the average of tests with the same test parameters.

[e] Only one test was done for this test parameter. The base plate bent about 0.5 inch and reuse of the base plate was very difficult.

Table 5.4. Static Test Results for T-bases (TB1-20 and TB3-20).

Test ID	Test Date	P.O. No.	Pole Dia., d_p (in.)	Square Base Plate Size		T.B.C. d_t (in.)	B.B.C. d_b (in.)	Breaking Moment (ft.-lb.)	Ultimate Moment Avg. of Three (ft.-lb.)	Location of Failure
				Width (in.)	Thk. (in.)					
TB1-20-38	12/22/96	616557	8	13.125	1.25	13.5	15.0	33,524[a]		Bottom tension corner
TB1-20-39	12/23/96	616557	8	13.125	1.25	13.5	15.0	43,506		Bottom tension corner
TB1-20-40	12/23/96	616557	8	13.125	1.25	13.5	15.0	44,830	44,405	Bottom tension corner
TB1-20-41	12/23/96	616557	8	13.125	1.25	13.5	15.0	44,879		Bottom tension corner
TB3-20-53	12/27/96	612280	9.5	15.125	1.25	15.0	17.0	52,684[b]		Buckled at mid depth on the compression side[b]
TB3-20-54	12/28/96	612280	9.5	15.125	1.25	15.0	17.0	48,329		Top tension corner
TB3-20-55	12/28/96	612280	9.5	15.125	1.25	15.0	17.0	47,034	47,876	Top tension corner
TB3-20-56	12/29/96	612280	9.5	15.125	1.25	15.0	17.0	48,265		Top tension corner

Note : 1 inch = 25.4 millimeters 1 ft-lb = 1.356 N-m.

[a] Breaking moment from this test is not within 10% of the average of tests with the same test parameters.

[b] This TB3-20 sample showed buckling phenomena during loading. It started buckling at 52,684 ft-lb moment and it cracked only during unloading at same location of buckling.

Table 5.5. Static Test Results for T-bases (TB3-17).

Test ID	Test Date	P.O. No.	Pole Dia., d_p (in.)	Square Base Plate Size		T.B.C. d_t (in.)	B.B.C. d_b (in.)	Breaking Moment (ft.-lb.)	Ultimate Moment Avg. of Three (ft.-lb.)	Location of Failure
				Width (in.)	Thk. (in.)					
TB3-17-42	12/24/96	615643	9.5	15.125	1.25	15.0	17.0	36,704[a]		Top tension corner
TB3-17-43	12/24/96	615643	9.5	15.125	1.25	15.0	17.0	54,140		Bottom tension corner
TB3-17-44	12/24/96	615643	9.5	15.125	1.25	15.0	17.0	47,504[a]	41,453	Bottom tension corner
TB3-17-45	12/25/96	615643	9.5	15.125	1.25	15.0	17.0	51,421		Top tension corner
TB3-17-46	12/25/96	615643	9.5	15.125	1.25	15.0	17.0	40,153[a]		Top tension corner
TB3-17-47	12/25/96	616601	9.5	15.125	1.25	15.0	17.0	43,376		Top tension corner
TB3-17-48	12/26/96	616601	9.5	15.125	1.25	15.0	17.0	41,691	42,485	Top tension corner
TB3-17-49	12/26/96	616601	9.5	15.125	1.25	15.0	17.0	42,388		Top tension corner

Note : 1 inch = 25.4 millimeters 1 ft-lb = 1.356 N-m.

[a] Breaking moments from all five tests for TB3-17 with purchase order no. 615643 differed by more than 10% from the average. So lower three test results were considered to calculate the average.

Table 5.5. (Continued)

Test ID	Test Date	P.O. No.	Pole Dia., d_p (in.)	Square Base Plate Size		T.B.C. d_t (in.)	B.B.C. d_b (in.)	Breaking Moment (ft.-lb.)	Ultimate Moment Avg. of Three (ft.-lb.)	Location of Failure
				Width (in.)	Thk. (in.)					
TB3-17-50	12/26/96	616601	9.5	15.125	1.25	15.0	15.0	34,749		Bottom tension corner
TB3-17-51	12/26/96	616601	9.5	15.125	1.25	15.0	15.0	35,121	35,034	Bottom tension corner
TB3-17-52	12/26/96	616601	9.5	15.125	1.25	15.0	15.0	35,234		Bottom tension corner
TB3-17-57	1/5/97	616601	9.5	15.125	1.50	15.0	17.0	53,296[b]		Top tension corner
TB3-17-58	1/5/97	616601	9.5	15.125	1.50	15.0	17.0	45,324		Top tension corner
TB3-17-59	1/6/97	616601	9.5	15.125	1.50	15.0	17.0	48,792	45,665	Top tension corner
TB3-17-60	1/6/97	616601	9.5	15.125	1.50	15.0	17.0	42,880		Top tension corner
TB3-17-61	1/6/97	616601	9.5	15.125	1.50	15.0	17.0	53,261[b]		Top tension corner

Note : 1 inch = 25.4 millimeters 1 ft-lb = 1.356 N-m.

[b] Breaking moment from this test was not within 10% of the average of tests with the same test parameters. So lower three test results were used to calculate the average.

with the key dimensional parameters held constant. The only factor that consistently controlled the tensile fracture location was the diameter of the top or bottom bolt circle. Whenever either bolt circle, top or bottom, was at its minimum value while the other one was at its maximum value, the failure always occurred near the bolt circle which was at its minimum value.

One test, TB3-20-53, exhibited a very unusual failure mode. It did not fail with a tensile fracture but had a buckling mode failure at mid height of the t-base on the compression side.

5.3 DETERMINATION OF MATERIAL PROPERTIES OF T-BASES

Three specific material properties of the t-base that were investigated are, Young's modulus of elasticity, tensile strength, and Rockwell hardness number. From each t-base, three flat test specimens were cut for the determination of tensile strength and modulus of elasticity. The test coupons provided by the manufacturer along with each t-base were not used because of the following reasons,

1. It was desirable to find the variation in modulus of elasticity, ultimate tensile strength of aluminum in the t-base. Hence test specimen were required from the actual t-base to find their properties.
2. To find the modulus of elasticity, it was required to attach strain gages or extensometer on the test coupon, which required a flat surface of at least one inch width.
3. A minimum of three test coupons were required from each t-base to check repeatability of test values and only one coupon was cast with each t-base.

5.3.1 Preparation of Tension Test Specimens

It was decided to cut a panel from one of the flat sides of the t-bases where the material had not failed or subjected to elastic plastic behavior. The flat piece was further cut into tension test and hardness test specimens. Various saws were used to cut a panel from the t-base, and their overall efficiency compared. A 184.15 mm (7-1/4 in) circular saw was found to be the most efficient both in speed and ease. A panel of size approximately 254 mm by 203 mm (10 in by 8 in) was cut from one of the flat side walls adjacent to the door opening. The flat surface opposite to the door could not be used as it had a hole in the center. From the cut panel, three strips of size, approximately 230 mm by 38 mm (9 in. by 1.5 in) were cut using a band saw. The remaining part was used to cut hardness test specimens, a test described later in this chapter. All specimens were specifically designated to the purchase order and type etc.

The cut strips were milled using a miller machine so as to make the sides parallel, smooth and a consistent width of 31.75 mm (1.25 in)($\pm$ 5%). The final dimensions of the test specimen were 229 mm by 31.75 mm (9 in. by 1.25 in). The difference in the thickness of the specimen varied between 0.254 and 0.381 mm (0.010 and 0.015 in); and

therefore the thickness was measured at three locations at ¼, ½ and ¾ along the length of the specimen and an average thickness was use in the calculations..

5.3.2 Test Procedure

The test specimen was fastened to the load frame of the MTS Universal Testing Machine with each end inside the grips. With the help of rubber bands, an extensometer was set up on the specimen at the center. The locking pin in the extensometer was removed and the initial apparent strain reading was recorded. Load was applied slowly, from zero in steps of 2,224 N (500 lbs) until 8,896 N (2000 lbs) and there after in steps of 1,780 N (400 lbs) until 25,000 N (5000 lbs). Since the machine is set up to operate on a load control condition, the loading could be stopped at a certain load and the strain reading recorded for the corresponding load. After reaching near 25,000 N (5000 lbs), the loading was stopped and the extensometer was removed from the specimen. This was done to avoid damage to the extensometer in the event of sudden failure of the specimen. Thereafter, the loading was continued until the specimen failed in tension. The machine automatically records the failure load which gives the tensile strength; the strains and their corresponding loads give the stress-strain curve and the modulus of elasticity.

5.3.3 Results of Material Properties from Tension Tests

All results from the tests for tensile strength and modulus of elasticity, in relation to the type of the t-base and the purchase order number are recorded in Appendix A. The results vary from one sample to the other. This indicates the variability that exists in the t-base samples. The average values of tensile strength and the modulus of elasticity for each type of t-base is shown in Table 5.6. It is worth noting from Table 5.6 that the average tensile strength obtained from the tests for TB1-17 is 238.87 Mpa (34,644 psi), which is much lower than 282.7 Mpa (41,000 psi), as provided by the manufacturer and as recorded in Table 5.7.

5.3.4 Rockwell Hardness Test

The aim of hardness test was to find out if there is any variation in the surface hardness of the t-base material and to investigate if there exists a correlation between the hardness number and the moment capacity. The hardness test was performed according to the ASTM Standards. As explained earlier, a panel was cut from the t-base and tension test specimens were cut from it. From the remaining part, a hardness specimen of size 76.2 mm by 63.5 mm (3 in. by 2 ½ in) was cut from each t-base to conduct a hardness test. This was to allow sufficient space between each of the five indentations made.

5.3.5 Test Procedure

Since the outer surface of the t-base was comparatively smoother than the inner surface, the outer surface was used to make indentations for the hardness test as it would give better results. The specimen was indented with the diamond bit at five different locations with minimum distance as specified by ASTM E18 and the hardness values

Table 5.6 Variation of Material Properties of T-bases

Material Property	Type of T-base			
Average Values	**TB1-17**	**TB1-20**	**TB3-17**	**TB3-20**
Average Tensile Strength, psi	34,644	32,588	34,757	35,947
Average Modulus of Elasticity, psi	1.064E+07	1.050E+07	1.007E+07	1.013E+07
Average Rockwell Hardness Number	46	46	49	45
Minimum Values				
Minimum Tensile Strength, psi	27,320	28,454	27,745	34,209
Minimum Modulus of Elasticity, psi	8.675E+06	9.180E+06	8.050E+06	9.251E+06
Minimum Rockwell Hardness Number	26	38	39	38
Maximum Values				
Maximum Tensile Strength, psi	39,381	36,017	37,956	37,857
Maximum Modulus of Elasticity, psi	1.200E+07	1.133E+07	1.150E+07	1.063E+07
Maximum Rockwell Hardness Number	61	52	56	51

Table 5.7 Mechanical Properties of T-bases Furnished by the Manufacturer

Supplier	P.O. No.	T-base ID	Tensile Strength (psi)	Yield Strength (psi)	Elong.% in 2 in.
JEM	616582	TB1-17	41,000	32,500	6
A-1 Ind.	615643	TB1-17	37,000	29,000	4
A-1 Ind.	616576	TB1-17	37,550	30,000	5
John K. Ind.	616544	TB1-17	Unavailable		
A-1 Ind.	615643	TB3-17	39,500	29,950	5
A-1 Ind.	616601	TB3-17	38,000	30,000	5
A-1 Ind.	616557	TB1-20	41,000	34,000	6
A-1 Ind.	612280	TB3-20	41,000	32,500	6

Note : 1 psi = 6.895 kPa

recorded. The machine was calibrated each time before and after test on each specimen, using a standard hardness specimen whose hardness was known.

5.3.6 Results of the Hardness Tests

The results of the hardness tests are reported in Appendix B. The rockwell hardness number varies from 26 to 61, 38 to 52, 39 to 56 and 38 to 51 and the average hardness values are 46, 46, 49 and 45 for TB1-17's, TB1-20's, TB3-17's and TB3-20's, respectively. The variation of hardness is shown in Table 5.6. No relation between hardness and the moment capacity of the T-Bases was discovered.

6. VALIDATION OF FINITE ELEMENT MODEL

6.1 Introduction

The load orientation corresponding to DDT (Door in Diagonal Tension) was found to be most critical as far as the t-base is concerned. Hence, load orientation DDT should control the design of the overall light pole/t-base system and the remainder of this project is restricted to the DDT load orientation. Here, a detailed description of finite element modeling of the light pole and other refinements incorporated into the existing model are given. The finite element model so constructed is analyzed and the strains obtained from the analysis are compared with the strains measured from the experimental setup.

6.2 Modeling of the Light Pole

In the finite element model discussed in Chapter 4 for the determination of critical load orientation, the loading was applied in the form of series of concentrated loads at the circumference of the base plate. The light pole was not included in that model. After close examination of the finite element results and the deflected behavior of the t-base/ base plate, it was found convenient to apply the load on the pole in the form of pressure loading instead of a series of concentrated loads at the inside circumference of the base plate. For this purpose, a small portion of the pole had to be modeled. Also, modeling of pole makes the finite element model a complete simulation of the actual t-base/light pole/base plate system existing in the field. The results obtained from both forms of loading were compared and were found to be matching quite well. Hence, it was decided to include the pole in all the subsequent studies of this research. The modified model is shown in Figure 6.1.

A three dimensional solid eight noded brick element was chosen to model the pole to maintain the compatibility between the base plate and the pole. The pole was inserted through a hole in the base plate and connected only at the top and bottom of the base plate. The portion of the pole inside the base plate was not connected to the base plate. This was simulated in the finite element model by providing common nodes to the pole and the base plate at the top and bottom only. The portion of the pole inside the base plate was provided with duplicate nodes. The welding of the base plate to the pole was simulated by means of 6-noded wedge solid elements to match the already existing finite element mesh of the base plate and pole. The total number of degrees of freedom for the entire t-base/base plate system was about 40,000 and 50,000 for TB1-17 and TB3-17, respectively. A moment equal to 40,680 N-m and 67,800 N-m (30,000 and 50,000 ft-lb) was applied on top of the pole in the form of equivalent pressure loading for TB1-17 and TB3-17, respectively. This applied pressure varied from a maximum at the extreme fiber to zero at the neutral axis. The deformed t-base model under the applied moment is shown in Figure 6.2.

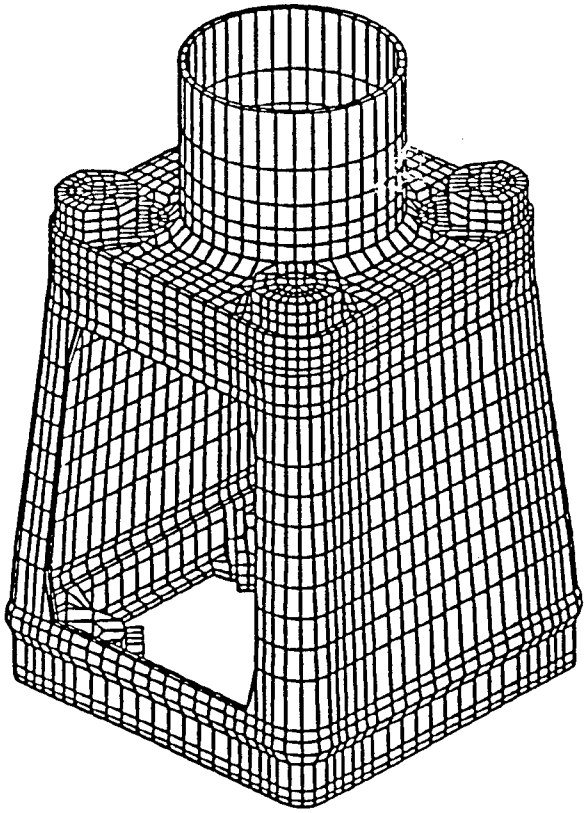

Fig.6.1 Finite Element Idealization of T-base/Light Pole System

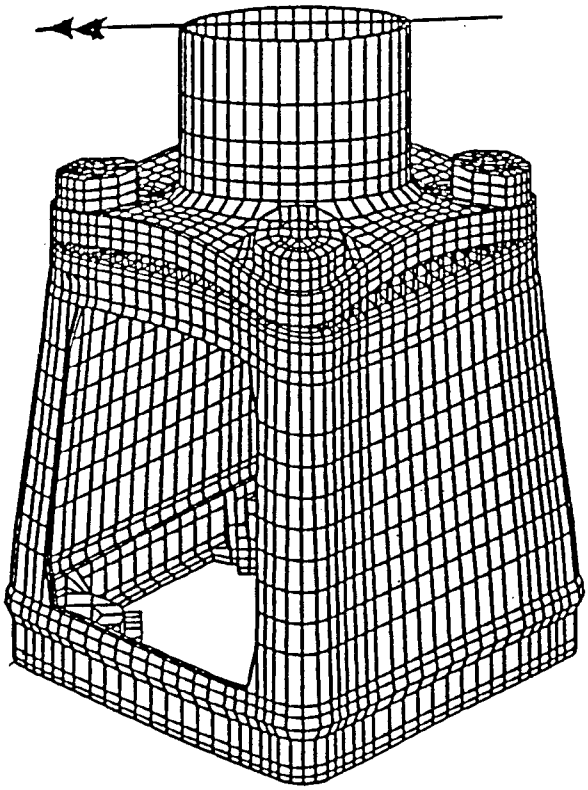

Fig. 6.2 Enlarged Deformation of T-base/Light Pole System

6.3 Thickness of T-base Shell

As discussed in Chapter 4, the thickness of the t-base shell was initially assumed to be 6.35 mm (0.25 in). uniform through out except at locations where it was possible to measure from outside as accurately as possible. In order to improve the finite element model, it was essential to know the exact thickness of the t-base at every location. One of the actual t-bases was cut at different sections to allow accurate thickness measurements to be taken. It was surprising to note that the t-base had different thickness at various sections. This could not be noticed had the t-base not been cut. This helped in understanding the geometric variations of the t-base. The thickness of the t-base shell varied in both horizontal and vertical directions. The variation in the horizontal direction was between 4.32 to 10.67 mm (0.17 to 0.42 inches) while the variation in vertical direction was from 4.32 to 6.35 mm (0.17 to 0.25 inches). All these thicknesses were incorporated into the finite element model as accurately as possible.

6.4 Contact Surfaces not Welded Within the T-base

T-bases are made of cast aluminum and have a welded joint at the interface of the bottom portion and the top portion of the t-base. In the initial finite element model, it was assumed that there was full contact between these two portions of the t-base and that they were fully welded together. However, the cut portion of the t-base revealed that the welding was continuous only on the outside surface. On the inside, the two portions were only welded in the curved regions of the corners. The finite element model was then modified to represent this changed condition. Common nodes were provided in the region of welding between the two portions and duplicate nodes were provided where there was no welding.

6.5 Modeling of Side Opening (Door)

The initial model used a uniform material thickness around the door opening. A cross section of the t-base cut horizontally across the door provided additional information that the thickness was not uniform. The material near the door was significantly thicker than locations far away from the door. The edges of the door were strengthened by providing more material. This could be attributed to the fact that the stress concentrations around the corners of the door will be larger. In order to reduce these levels of stress concentrations around the door, the manufacturer has implemented two geometric features.

1. Increased thickness near the door
2. Rounded corners were provided as smooth transitions between sides of the door at the corners. In the modified finite element model, all these aspects were incorporated.

6.6 Validation of Finite Element Results

Finite element analyses were conducted after incorporating all the modifications listed above into the model and the results were compared with the static tests conducted in the laboratory. The following parameters were selected for comparing the test data with the finite element analysis results.

1. Top Bolt Circle Diameter = 342.9 mm (13.5 in)
2. Bottom Bolt Circle Diameter = 381 mm (15 in)
3. Base Plate Thickness = 32 mm (1.25 in)
4. Pole Diameter = 203.2 mm (8 in)

The complete finite element idealization of the t-base, base plate and pole along with top and bottom bolts is shown in Figure 6.1. The overall deformation of the entire structure is shown in Figure 6.2. The maximum principal stresses in the t-base and base plate are considered to be most critical for the design of t-base. Hence, the maximum principal stresses are obtained from the post processing feature of FEMAP. FEMAP provides the maximum principal stresses in two forms. One is in the form of contour plots and the other in the form of X-Y plots. It is very difficult to obtain the absolute maximum principal stress from the contour plots since the stresses are given in the form of different colors and each color representing a particular range. Where as, X-Y plots will give the maximum principal stresses in each element. Hence, it is very convenient to obtain the absolute maximum principal stress from these plots and the X-Y plots were used in this research. Validation of the results will be discussed in the following section.

One of the main goals of this experiment was to measure the strains induced by the applied moments at some selected critical locations in the base plate as well as in the t-base. Four strain gages were placed on the steel base plate at the center of each of the four sides and four additional strain gages were placed on the t-base. The strategic locations and orientations of the strain gages were determined from results of the finite element analysis. Since the load orientation corresponds to DDT, two strain gages were placed at the extreme tension and compression fibers on each side of the t-base one at the top and one at the bottom of the t-base. In order to capture the strains at the critical locations of the t-base, gages 9 and 10 were placed on the top and bottom of the tension side, respectively. Similarly, gages 12 and 13 were placed on the top and bottom of the compression side, respectively, exactly opposite gages 9 and 10, respectively.

6.7. Comparison of Strains with Experiments

The strains measured from the base plate and t-base were compared with those obtained from the finite element analysis. The results are discussed separately in the following paragraphs.

6.7.1 Comparison of Strains in the Base Plate

The strains in the base plate from gages 6 and 7 are shown in Figures 6.3 and 6.4, respectively. Several tests were conducted to get consistency from the results. The strains obtained from these tests were plotted along with the strain predicted by the finite

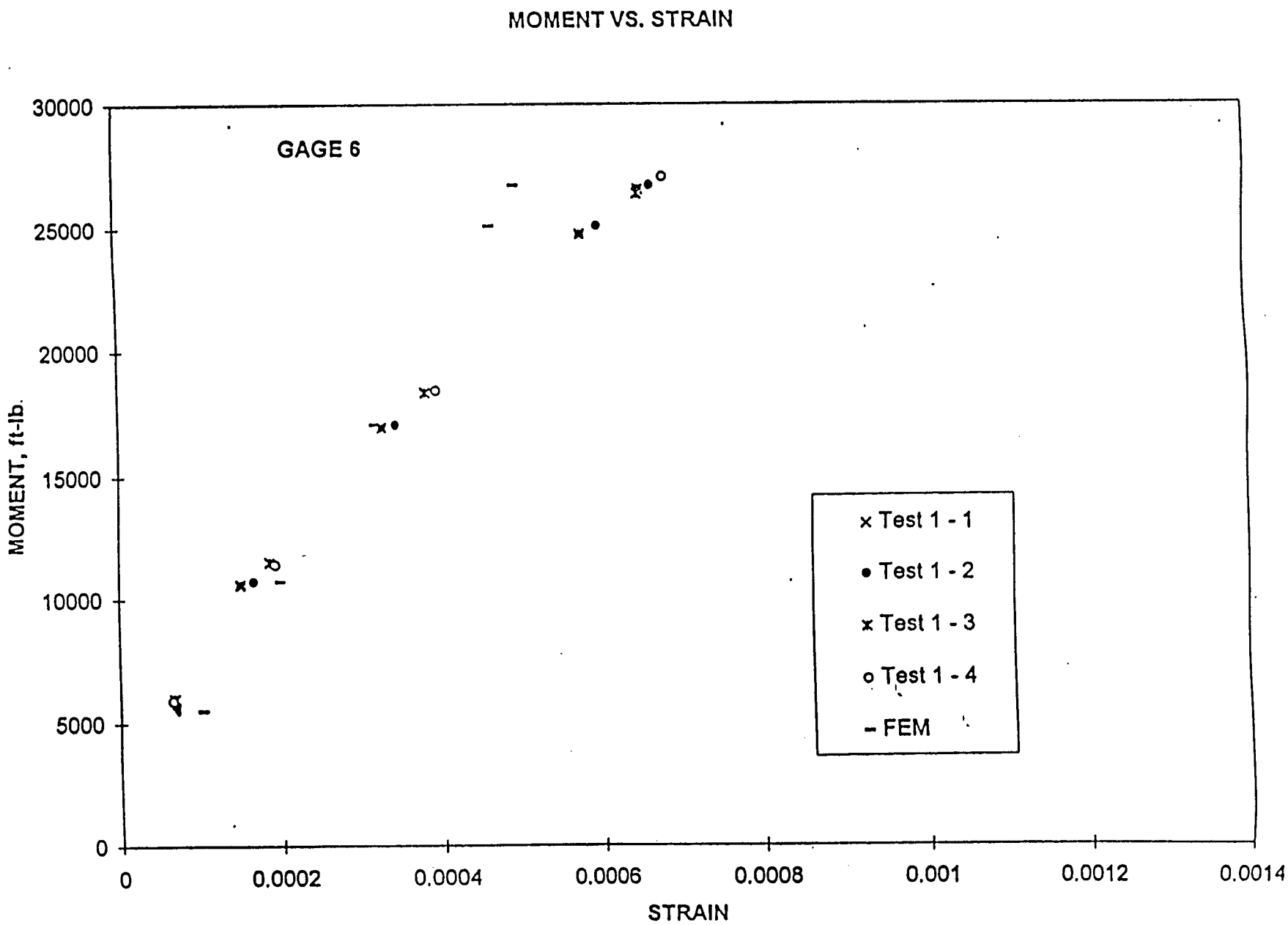

Fig. 6.3 Comparison of Strains in the Base Plate at Gage Location 6

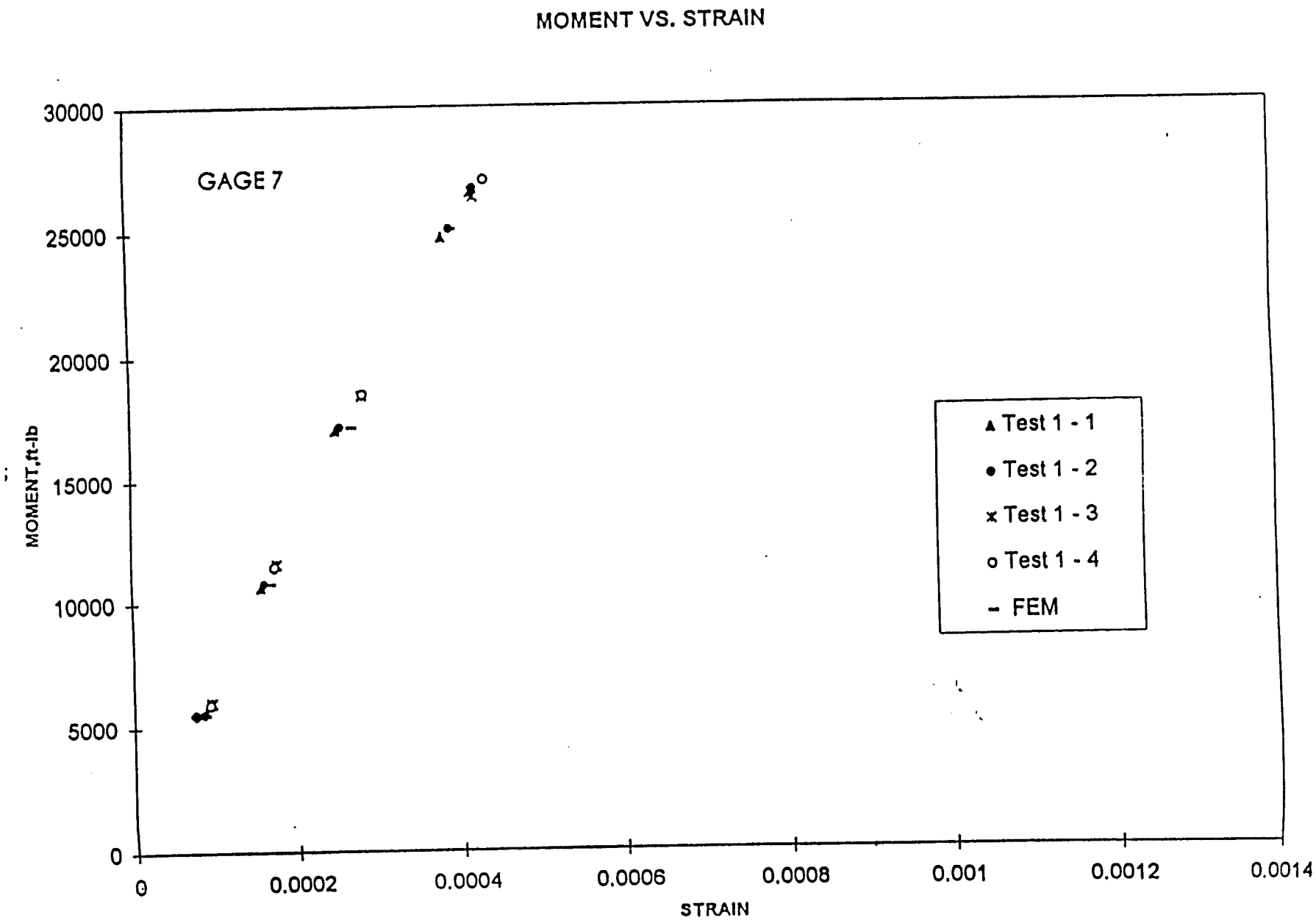

Fig. 6.4 Comparison of Strains in the Base Plate at Gage Location 7

element analysis. It can be seen from these figures that the measured experimental strains in the base plate and strains from the finite element analysis matched well.

6.7.2 Comparison of Strains in the T-Base

The strains in the t-base collected from gages 9, 10, 12, and 13 are compared to strains predicted by the finite element analysis in Figures 6.5, 6.6, 6.7, and 6.8 respectively. From these figures, it can be seen that the correlation between measured and predicted strains varied with location on the t-base. Gage 9, located at the top tension corner of the t-base, shows good and slightly conservative correlation. Gage 12, located at the top compression corner of the t-base, shows good but slightly unconservative correlation. Gages 10 and 13, located on the bottom tension and bottom compression side of the t-base, respectively, do not show very good correlation. However, it is important to note that for both of the locations on the tension side of the t-base, which are the critical locations for predicting tensile fracture of the brittle material, the finite element analysis predicted conservative results.

Possible reasons for the varied correlation between the predicted and measured strains were considered and a discussion of those reasons is provided in the following section.

1. The modulus of elasticity of the base plate, made of 36 grade steel, is very well known. Hence, the material model for the steel base plate with its homogeneous characteristics was fairly accurate. This is reflected in the close correlation between the analytical and experimental strains in the base plate as seen in Figures 6.3 and 6.4. The modulus of elasticity of the material of the t-base which was made of cast aluminum was not known exactly and from later experiments it was found that the value of modulus of elasticity of t-base material varied between 55.16 Gpa and 75.85 Gpa (8 and 11 million psi). The modulus of elasticity of the cast aluminum t-base was taken as 73.78 Gpa (10.7 million psi) in the finite element analysis as suggested in many standard text books. This value was also assumed to be constant for the entire aluminum t-base in the FEM analysis but perhaps, it could vary at different locations in the t-base.
2. The thickness of the t-base was not constant but varies through out the t-base and could not be modeled exactly. An average thickness was used in general regions of the t-base. In addition, there are many rounded corners and fillets through out the t-base which had to be modeled as sharp corners.
3. Another important characteristics observed in the t-base was that the welding between the top and bottom parts of the t-base was not uniform. This welded joint is located near the bottom of the t-base where the correlation between the measured and predicted strains was the poorest. The non-uniformity of the weld could cause slight variations in the stress distribution in the t-base and could account for the poor correlation in that region.

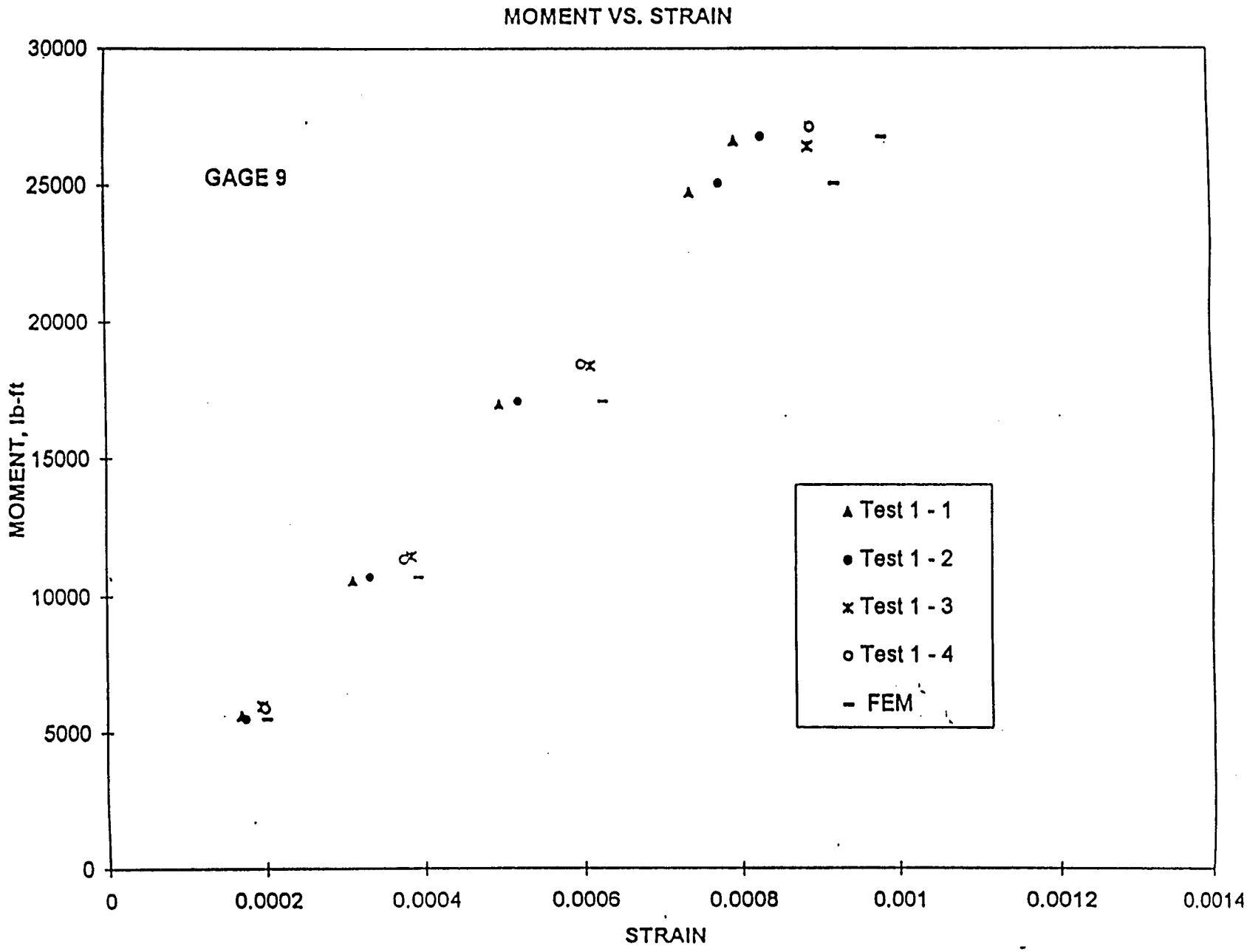

Fig. 6.5 Comparison of Strains in the Base Plate at Gage Location 9

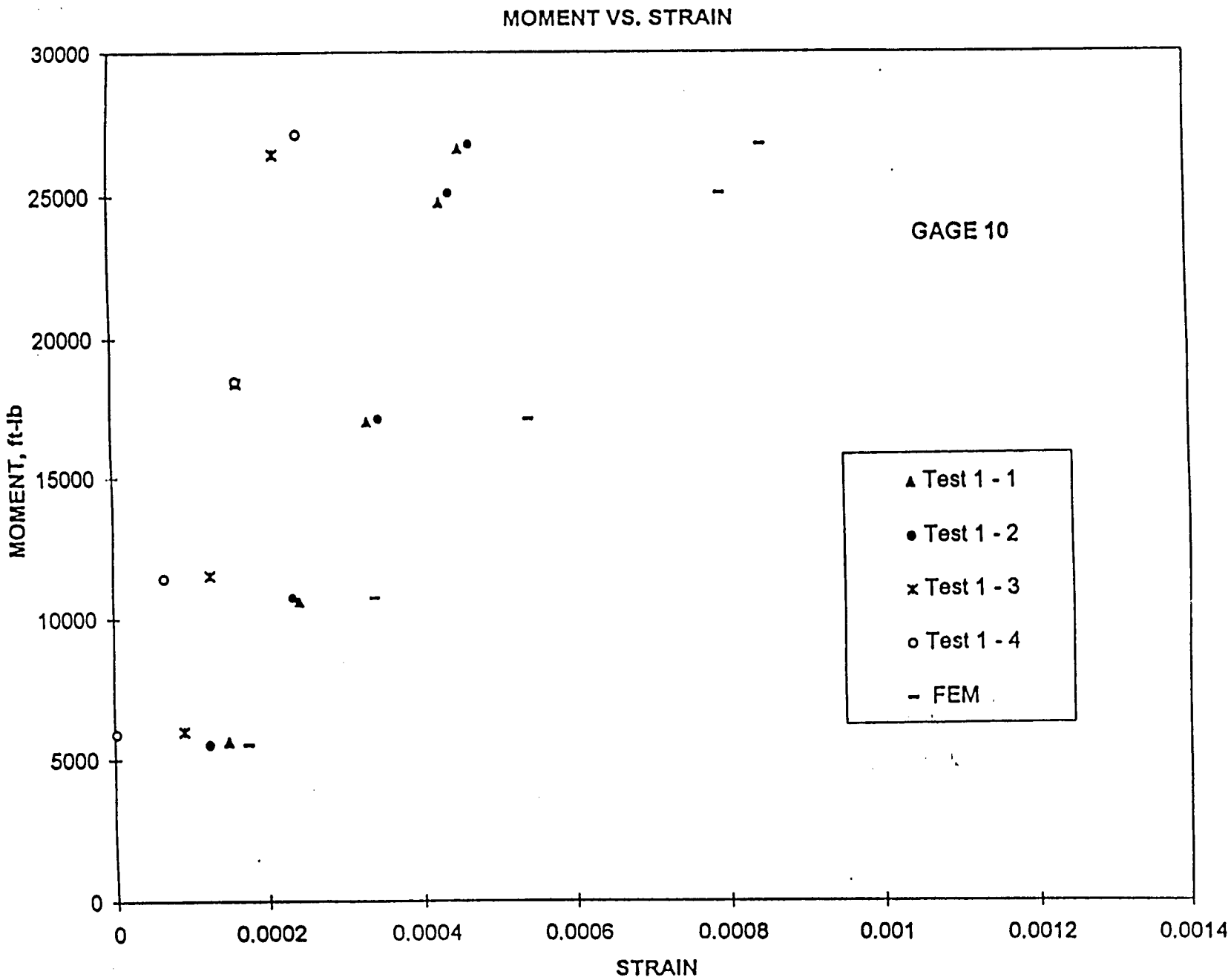

Fig. 6.6 Comparison of Strains in the Base Plate at Gage Location 10

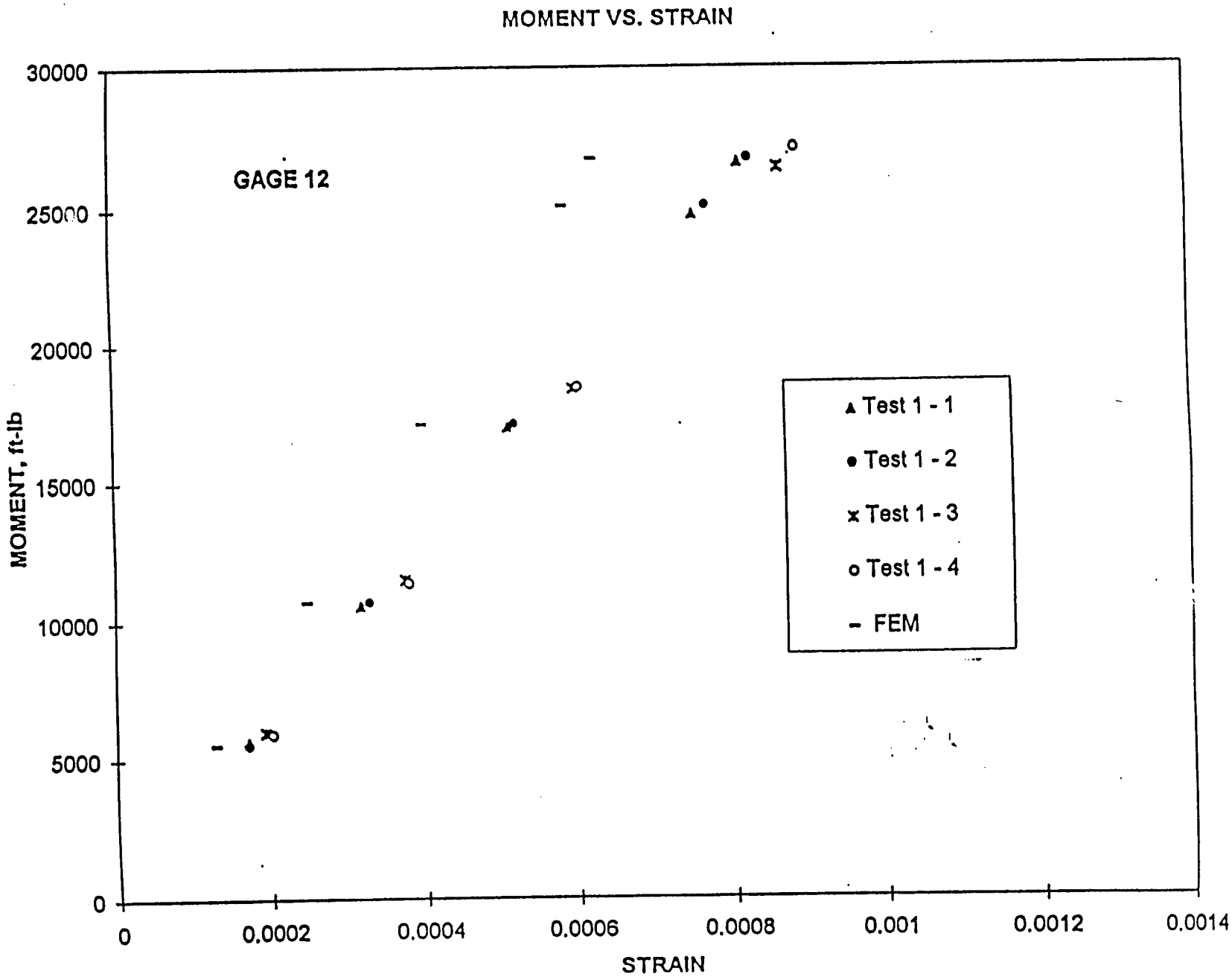

Fig. 6.7 Comparison of Strains in the Base Plate at Gage Location 12

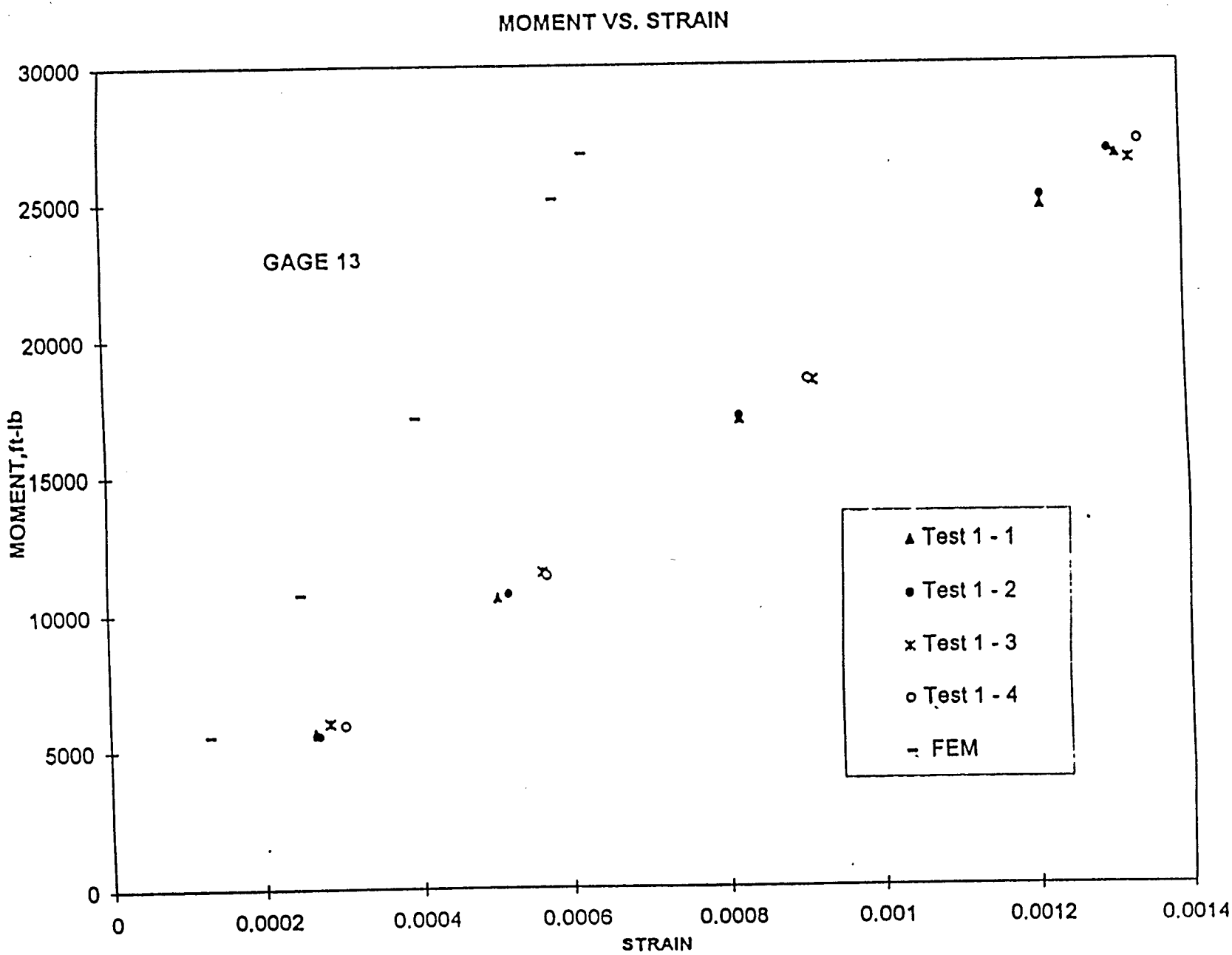

Fig. 6.8 Comparison of Strains in the Base Plate at Gage Location 13

4. In the finite element model, an eight noded brick element was employed as the primary element. This element, even though it gives fairly good answers in membrane action, has a slightly stiffer characteristic for bending which could account for the poorer correlation. To increase the accuracy of the finite element solution, a higher order element could be used or multiple eight noded elements could be used to model the thickness. Either of these solutions would result in too many degrees of freedom and would be too complicated for developing the discretized model.
5. The connection between the t-base and the test frame was not modeled exactly but was modeled to yield a conservative finite element solution. This conservative variation in modeling could also account for the poorer observed correlation of strain in the lower region of the t-base.

These are possible explanations for the poorer observed correlation between the measured and predicted strains in the cast aluminum t-base. It is import to note again that the finite element analysis always predicted higher strains in the tension regions of the t-base which is a conservative solution since tensile fracture if the controlling failure mechanism. Because of this, the finite element method can be used to predict the ultimate moment capacity of the t-bases.

6.8 Nonlinear Behavior of the T-Base and the Base Plate

It was observed during some of the tests that the steel base plate underwent some slight elasto-plastic deformation, thus making the interaction between the base plate and t-base more complicated. Besides, the t-base itself will undergo some elasto-plastic deformation before failure as observed in the uniaxial experimental stress test. This nonlinear phenomena could not be studied in the present finite element model using the CSA Nastran. To understand the behavior completely in the nonlinear range, a non linear finite element analysis with material non linearity was required. A nonlinear finite element computer code called GENSA was used for this purpose. This code is an explicit code and for the given number of degrees of freedom and gap elements, the code did not function as well as hoped.

6.9 Validation and Calibration of the Finite Element Models

The finite element models developed in this study were calibrated and their results verified prior to their use in this study. These finite element models cannot account for the variabilities which occur in the t-bases and which effect their ultimate moment capacities (M_u). These variabilities are caused by non-homogeneous material properties and fabrication techniques such as casting, heat treating, and welding. These variabilities can be seen by reviewing the moment capacity test data provided in Table 5.3 or Table A.4. Ultimate moment capacities ranged from 47,405 to 65,968 N-m (34,960 ft-lb to 48,649 ft-lb) for tests TB1-17-5 through TB1-17-16 with all the dimensional parameters held constant. Variations in the moment capacities can be seen between t-bases bought at the same time (having the same purchase order number) as well as between t-bases bought a

different times (having different purchase order numbers). Similar ultimate moment capacity variability can be seen for tests TB3-17-42 through TB3-17-49 which ranged from 49,771 to 73,414 N-m (36,704 ft-lb to 54,140 ft-lb). These variabilities were accounted for in the finite element models by calibrating the models using the full scale test data. The ultimate tensile strength (F_u) of the cast aluminum material was determined for each t-base tested and a comparison was made to try to find a correlation between F_u and M_u of each t-base tested. No consistent correlation was found between these two properties indicating that the variability of M_u found between t-bases with constant dimensional parameters came at least partially from one of the other sources discussed above. Even though no consistent correlation was found between F_u and M_u, F_u was found to be the easiest property to use to calibrate the finite element models using the experimental data.

T-base failure was assumed to occur during a finite element analysis when the maximum principle stress in the cast aluminum exceeded F_u of the material. The moment applied to the t-base which caused the maximum principle stress to reach F_u was set as M_u of the t-base. Since a linear finite element analysis was used in this study, constant moments of 40,680 and 67,800 N-m (30,000 ft-lb and 50, 000 ft-lb) was applied to each TB1-17 and TB3-17 t-base model, respectivley, and the maximum principle stress was determined in the cast aluminum. M_u was then determine using the following linear relationship:

$$M_u = F_u * (M_a) / \sigma_{max}$$

where M_a is the applied moment and σ_{max} is the maximum principle stress in the aluminum caused by the applied moment M_a. To calibrate the finite element models to yield lower bound solutions when compared to the experimental data, values for F_u were selected as 248.22 Mpa and 206.85 Mpa (36,000 psi and 30,000 psi) for the TB1-17 and TB3-17 models, respectively. It can be seen by a review of the data provided in Table A.4 that the finite element analyses did indeed yield a lower bound value of M_u when compared to the average experimental M_u for each parameter set.

7. CORRELATION OF FEM WITH EXPERIMENTS

7.1 Introduction

Full scale experimental and finite element parametric studies were conducted to investigate the effect of each dimensional parameter separately on the ultimate moment capacity of the t-base. Dimensional parameters and measured moment capacities from the full scale tests are provided in Tables 5.3 to 5.5, while dimensional parameters and associated predicted moment capacities from the linear finite element analyses are provided in Table 7.1 and Table 7.2 for TB1-17's and TB3-17's, respectively. It should be noted that finite element parametric studies are all encompassing with M_u being determined with each of the four dimensional parameters set at their minimum and maximum practical limits. This resulted in 16 finite element analyses for each t-base model, TB1-17 and TB3-17. On the other hand, project funds limited the number of full scale tests to a selected number of parametric values. However, sufficient number of full scale tests were conducted to allow the study of each parameter's effect separately. The four dimensional parameters that were investigated in this study were:

1. Top bolt circle diameter (d_t)
2. Bottom bolt circle diameter (d_b)
3. Pole base plate thickness (t)
4. Pole diameter at base plate level (d_p)

The limit of each parameter used in this study are provided in Table 7.3 with the top and bottom bolt circle diameter set near the manufacture's recommended minimum and maximum limits. Pole diameters and base plate thickness were selected following a review of current pole manufacture's details.

7. 2 Effect of Top Bolt Circle

Experimental Test 6 to 9 and Test 17 to 20, Test 21 to 23 and Test 30, and Test 24 to 26 and Test 27 to 29 were conducted to evaluate the effect of the top bolt circle diameter on M_u of TB1-17's. It can be seen in the experimental test data that an increase in d_t, with the other parameters held constant, resulted in an increase in M_u. The amount of increase in M_u is dependent on the values of the other parameters but was as high as 44% in the experimental tests as d_t increased from its minimum to maximum value. Finite element analyses FEA 1 and 5, FEA 2 and 6, FEA 3 and 7, FEA 4 and 8, FEA 9 and 13, FEA 10 and 14, FEA 11 and15, and FEA 12 and 16 were conducted to study this effect on both the TB1-17 and TB3-17. Once again as seen in Tables 7.1 and 7.2, M_u increased as d_t increased in ever case. M_u increases as predicted by the finite element analyses was as high as 66% and 27% for TB1-17 and TB3-17, respectively.

The increase in M_u related to the increase in d_t is easily explained. One important key to remember is take the brittle cast aluminum t-bases fail on the tension side when the

Table 7.1 Results of the Finite Element Parametric Study for TB1-17

FEA Number	Key Parameters				Maximum Principal Stress, psi	Ultimate Moment, ft-lb
	d_b inches	d_t inches	d_p inches	t inches		
1	13	11	7	1.0	47,016	22,971
2	13	11	7	1.5	43,642	24,747
3	13	11	8	1.0	49,499	21,819
4	13	11	8	1.5	43,426	24,870
5	13	13.5	7	1.0	35,031	30,830
6	13	13.5	7	1.5	34,952	30,899
7	13	13.5	8	1.0	36,991	29,196
8	13	13.5	8	1.5	36,875	29,288
9	15	11	7	1.0	46,333	23,310
10	15	11	7	1.5	43,702	24,713
11	15	11	8	1.0	49,232	21,937
12	15	11	8	1.5	40,556	26,630
13	15	13.5	7	1.0	27,887	38,727
14	15	13.5	7	1.5	26,580	40,632
15	15	13.5	8	1.0	30,560	35,340
16	15	13.5	8	1.5	28,579	37,790

Note : The ultimate moment capacity of the TB1-17's was obtained by using the tensile strength of cast aluminum as 36 ksi.

1 inch = 25.4 mm 1 ft-lb = 1.356 N-m
1 psi = 6.895 kPa

Table 7.2 Results of the Finite Element Parametric Study for TB3-17

FEA Number	Key Parameters				Maximum Principal Stress, psi	Ultimate Moment, ft-lb
	d_b inches	d_t inches	d_p inches	t inches		
1	15	13	8	1.0	60,459	24,810
2	15	13	8	1.5	58,263	25,745
3	15	13	10	1.0	59,167	25,352
4	15	13	10	1.5	58,714	25,548
5	15	15	8	1.0	47,761	31,406
6	15	15	8	1.5	45,843	32,720
7	15	15	10	1.0	57,305	26,176
8	15	15	10	1.5	56,796	26,410
9	17	13	8	1.0	48,426	30,975
10	17	13	8	1.5	39,848	37,643
11	17	13	10	1.0	48,225	31,104
12	17	13	10	1.5	34,534	43,435
13	17	15	8	1.0	45,169	33,209
14	17	15	8	1.5	35,168	42,652
15	17	15	10	1.0	45,698	32,824
16	17	15	10	1.5	32,811	45,716

Note : The ultimate moment capacity of the TB3-17's was obtained by using the tensile strength of cast aluminum as 30 ksi.

1 inch = 25.4 mm 1 ft-lb = 1.356 N-m
1 psi = 6.895 kPa

Table 7.3 Minimum and Maximum Limits of Parameters Studied

	d_t inches	d_b inches	d_p inches	t inches
TB1-17 (Test)	11.0 - 13.5	13.0 - 15.0	7.0 - 8.0	1.0 - 1.25
TB1-17 (FEM)	11.0 - 13.5	13.0 - 15.0	7.0 - 8.0	1.0 - 1.5
TB3-17 (Test)	15.0	15.0 - 17.0	9.5	1.25 - 1.5
TB3-17 (FEM)	13.0 - 15.0	15.0 - 17.0	8.0 - 10.0	1.0 - 1.5

Note: 1 inch = 25.4 mm

stress at any point in the material reaches it ultimate tensile strength. The bending moment caused by the transverse wind forces acting on the pole is transmitted from the pole base plate to the horizontal flange of the t-base via the bolt on the tension side. This moment must then be transmitted from the top flange of the t-base to the approximately vertical wall of the t-base. If the bolt were directly above the wall of the t-base, the moment would be transmitted only as an axial tensile stress into the aluminum t-base wall. However, the bolt is off-set from the t-base wall which causes an additional bending moment to occur in the t-base wall. It is the superposition of the axial tensile stress and the bending moment tensile stress which cause failure when their sum reaches the ultimate tensile strength of the material. As the top bolt circle increases, the moment arm in the top flange decreases which decreases that portion of the tensile stresses in the aluminum that is caused by bending. This allows an increase in moment applied to the t-base before the aluminum reaches its ultimate tensile strength and failure occurs. This concept is support by the location of the failure in the t-bases during full scale testing. The location of the failure occured on the tension side and varied between the juncture of the top and bottom flanges with the side wall through out the testing but always occurred at the top juncture when the smaller dt was used.

7.3 Effect of Bottom Bolt Circle

Experimental Test 6 to 9 and Test 35 to 37, and Test 24 to 26 and Test 31 to 34 were conducted to evaluate the effect of the bottom bolt circle diameter on M_u of TB1-17's. It can be seen in the experimental test data that an increase in d_b, with the other parameters held constant, resulted in an increase in M_u. The amount of increase in M_u is dependent on the values of the other parameters but was as high as 18% in the experimental tests as d_b increased from its minimum to maximum value. Experimental Test 47 to 49 and Test 50 to 52 were conducted to evaluate the effect of the bottom bolt circle diameter on M_u of TB3-17's. Results were similar with a 21% increase in M_u. Finite element analyses FEA 1 and 9, FEA 2 and 10, FEA 3 and 11, FEA 4 and 12, FEA 5 and 13, FEA 6 and 14, FEA 7

and15, and FEA 8 and 16 were conducted to study this effect on both the TB1-17 and TB3-17. Once again as seen in Tables 7.1 and 7.2, M_u increased as d_b increased in every case. M_u increases as predicted by the finite element analyses were as high as 31% and 73% for TB1-17 and TB3-17, respectively.

The explanation of the increase in M_u related to the increase in d_b is similar to that of the increase caused by d_t at the top of the t-base. The stresses in the top of the t-base wall are transmitted parallel to the wall to the bottom of the t-base where the must be transmitted through the bottom flange and into the foundation via the anchor bolts. Once again, it is superposition of the axial and bending moment tensile stresses at the juncture of the t-base wall and bottom flange which is the key. As d_b increases, the bottom flange moment arm decreases reducing the stresses in the aluminum caused by bending. this allows more moment to be applied to the t-base before failure occurs. Once again, the location of the failure supports this concept in that the failure always occurred at the bottom tension corner when the smaller d_b was used.

7.4 Effect of the Base Plate Thickness

Experimental Test 6 to 9 and Test 21 to 23, and Test 17 to 20 and Test 30 were conducted to evaluate the effect of the base plate thickness (t) on M_u of TB1-17's. Experimental Test 47 to 49 and Test 57 to 61 were conducted to evaluate the effect of the t on M_u of TB3-17's. It can be seen in the experimental test data, Table 5.3, Table 5.4 and Table 5.5, that an increase in t, with the other parameters held constant, resulted in an increase in M_u. The amount of increase in M_u is dependent on the values of the other parameters but was as high as 11% and 8% for TB1-17 and TB3-17, respectively. Finite element analyses FEA 1 and 2, FEA 3 and 4, FEA 5 and 6, FEA 7 and 8, FEA 9 and 10, FEA 11 and 12, FEA 13 and 14, and FEA 15 and 16 were conducted to study this effect on both theTB1-17 and TB3-17. Once again as seen in Tables 7.1 and 7.2, M_u increase as t increase in ever case. M_u increases as predicted by the finite element analyses were as high as 21% and 40% for TB1-17 and TB3-17, respectively.

The increase in M_u associated with the increase in t can be explained by considering the superposition of the tensile stresses at the juncture of the top flange and side wall of the t-base in-conjunction-with the interaction of the pole base plate and t-base top flange. Since the bending of the top flange of t-base and the pole base plate are interconnected due to the clamping action of the bolt that attaches these two parts, the tensile stresses that occur in the t-base side wall are effected by the stiffness of the pole base plate. The larger base plate thickness increases the stiffness of the base plate which reduces the amount of bending that occurs in the base plate and the top flange of the t-base. This reduces the amount of tensile stresses, caused by bending of the top flange, that occur in the t-base side wall which allows more moment to be applied to the t-base before the ultimate tensile strength of the aluminum is reached. Thus, we see the increase in M_u associated with the increase in t.

7.5 Effect of Pole Diameter

Experimental Test 6 to 9 and Test 24 to 26, Test 17 to 20 and Test 27 to 29, and Test 31 to 34 and Test 35 to 37 were conducted to evaluate the effect of the pole diameter on M_u of TB1-17's. It can be seen in the experimental test data that an increase in d_p, with the other parameters held constant, yielded mixed results in that 2 cases resulted in a 1% decrease in M_u while 1 case resulted in a 7% increase in M_u as the pole diameter increased from 177.8 to 203.2 mm (7 to 8. Inches). Finite element analyses FEA 1 and 3, FEA 2 and 4, FEA 5 and 7, FEA 6 and 8, FEA 9 and 11, FEA 10 and 12, FEA 13 and15, and FEA 14 and 16 were conducted to study this effect on both the TB1-17 and TB3-17. The finite element results Tables 7.1 and 7.2 also show mixed results with some increases and some decreases in M_u as d_p increased. Changes in M_u as predicted by the finite element models ranged from -10% to +8% for TB1-17 and from -20% to +15% for TB3-17.

Upon review of the parameters and associated values of M_u, no specific consistent correlation could be identified. However, several factors were identified which help explain the mixed results. The moment caused by transverse wind forces acting on the pole must be transferred from the pole base plate to the top flange of the t-base via the bolts connecting the two units. This load transfer mechanism is a complex interaction phenomena which is effected by the stiffness of the base plate. For a given top bolt circle diameter, as the pole diameter gets larger two things happen. First, the moment arm, that is causing bending in the base plate, between the outer edge of the pole and the bolt is getting smaller. This should cause less bending in the base plate and therefore result in an increased M_u value for the t-base. Second, the cross section of the base plate is getting smaller as the diameter of the pole is getting larger. This results in a reduced stiffness in the base plate causing more bending in the plate to occur which should result in a decreased M_u value for the t-base. The offsetting effect of these two factor helps to explain the mixed results of M_u as a function of d_p. In addition, the stiffness of the base plate which effects M_u is also effected by its thickness. Therefore, there are actually 3 major parameters which effect the value of M_u when we start considering the effect of d_p and it is their specific combinations and interactions which produce the mixed results seen in this portion of the study.

7.6 Interaction Effect of the Key Dimensional Parameters

The fact that the values of the key dimensional parameters, separately, significantly effect the ultimate moment capacity of the t-base was discussed above. The range of M_u for the TB1-17's was observed as 41,763 to 60,530 N-m (30,799 to 44,639 ft-lbs) and 29,587 to 55,097 N-m (21,819 to 40,632 ft-lbs) from the results of the full scale tests and finite element analyses, respectively, for the parameter ranges investigated. The range of M_u for the TB3-17's was observed as 47,506 to 61,922 N-m (35,034 to 45,665 ft-lbs) to 33,642 to 61,991 N-m (24,810 to 45,716 ft-lbs) from the results of the full scale tests and finite element analyses, respectively, for the parameter ranges investigated. However, the magnitude of the change in M_u for any given parameter varied depending on the values of

the other parameters which were being held constant. This indicates that there is an interaction between the parameters which must be considered when determining M_u. In an effort to combine all the dimensional parameter associated with the top of the t-base into a single non-dimensional parameter, an L/t ratio was developed and investigated. Here, L is the dimension from the edge of the pole to the centerline of the bolt in the base plate and t is the thickness of the base plate.

$$L = (d_t - d_p) / 2$$

$$L / t = (d_t - d_p) / (2 * t)$$

The ultimate moment capacities of the TB1-17's shown in Table 7.1 with bottom bolt circles of 330.2 mm (13 inches) were plotted against their corresponding L/t ratios as shown in Figure 7.1. This 3-dimensional box helps to visualize the effect that each top parameter, separately and corporately, has on M_u. Since each corner of the box represents one set of the key top dimensional parameters all set at one of their extreme limits, this figure could be used to determine M_u for any set of top parameters with a bottom bolt circle of 330.2 mm (13 inches). However, this interpolation process becomes cumbersome when more than one parameter is varied from their extreme limits. This process is further complicated since Figure 7.1 is only for a bottom bolt circle of. 330.2 mm (13 inches). A separate L/t verses M_u diagram would have to be constructed for d_b equal to 381 mm (15 inches) and an additional interpolation performed if d_b is set between its to extreme limits. To simplify this process, a computer code was developed which accounts for all of the key dimensional parameter and predicts the value of M_u associated with any set of values of key parameters for TB1-17 and Tb3-17. This code and its development are discussed in Chapter 8.

7.7 Strength Comparison of 1975 and 1985 AASHTO Standard T-bases

T-bases which were originally design to meet the 1975 AASHTO dynamic crash standard are 508 mm (20 inches) in height. In 1985, the AASHTO dynamic crash requirements were modified and required a more fragile t-base. The new t-bases which were designed to meet the 1985 AASHTO standard are 431.8 mm (17 in) height. One question that has arisen is whether or not the ultimate moment capacity, with respect to wind loads, of the more fragile t-bases which meet the 1985 AASHTO standard are as strong as their corresponding 1975 t-bases. This uncertainty causes maintenance and operation problems and higher associated cost. New construction proceeds using the 431.8 mm (17 in) t-bases while there is a large number of existing 508 mm (20 in) t-bases installed in the field. Current TxDOT policy is to replace knocked down poles with like kind t-bases. This means the TxDOT must maintain an inventory of TB1-17's, TB1-20's, TB3-17's, and TB3-20's which is more expensive and more confusing to field personnel. One objective of this project was to determine if damaged TB1-20's and TB3-20's can be replaced with TB1-17's and TB3-17's, respectively, yet provide adequate strength to resist wind induced forces and moments. Full scale test were conducted three sets of TB1-17's,

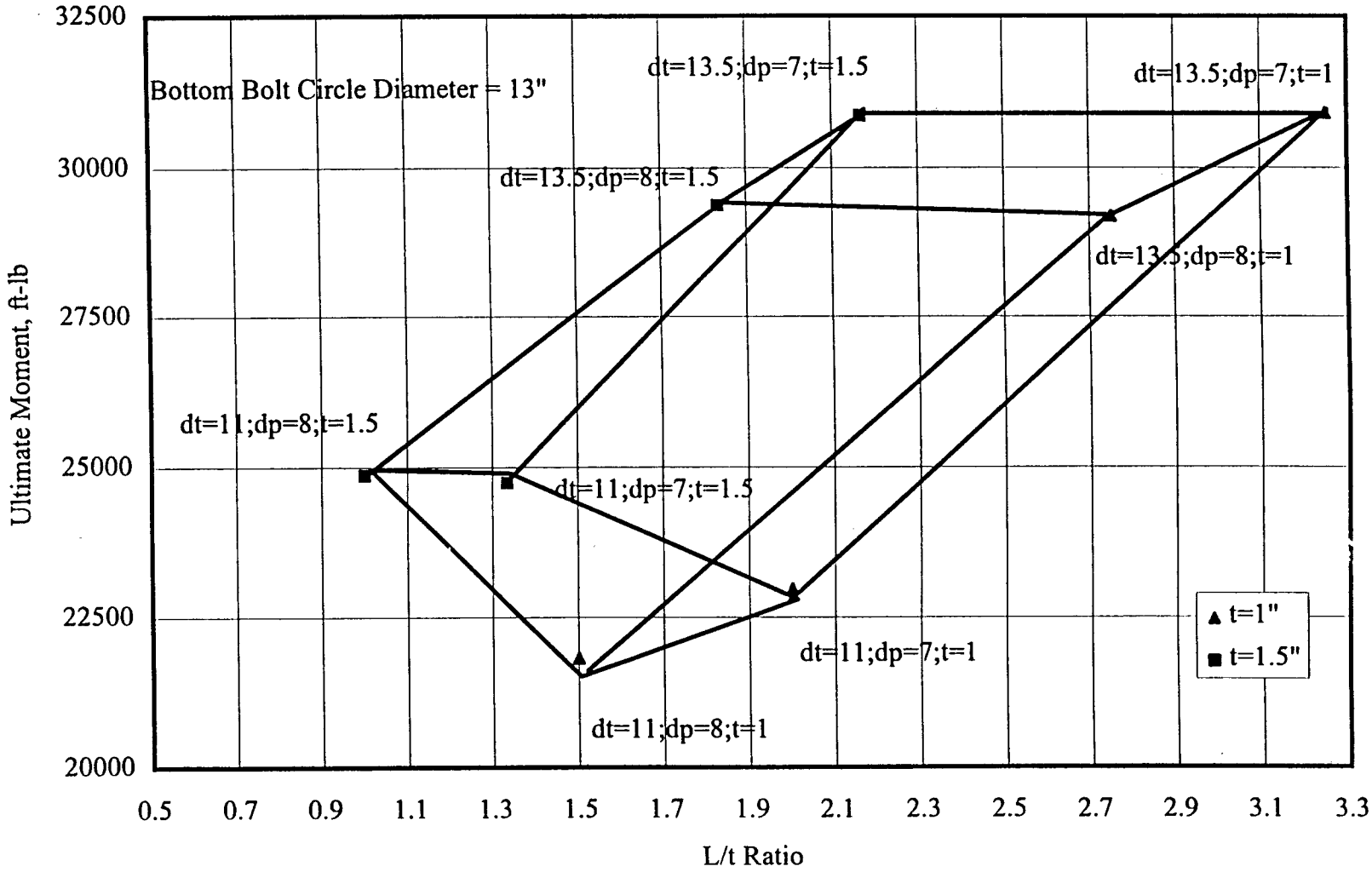

Figure 7.1 L/t Ratio VS Ultimate Moment L/t = 1/2 x (dt-dp)/t

Test 6 to 9 , Test 10 to 12, and Test 13 to 16, with constant parameters as shown in Table 5.3. Their corresponding ultimate moment capacity were determined as 59,945 N-m, 51,453 N-m, and 59,945 N-m (44,207 ft-lbs, 37,945 ft-lbs, and 44,214 ft-lbs) as shown in Table 7.4. For comparison, one set of TB1-20's, Test 38 to 41, was tested, with the same constant parameters, and their ultimate moment capacity was determined to be 60,213 N-m (44,405 ft-lbs). As can be seen, two sets of TB1-17's had capacities similar to the TB1-20's, yet one TB1-17 set was significantly weaker. In addition, full scale test were conducted two sets of TB3-17's, Test 42 to 46 and Test 47 to 49, with constant parameters as shown in Table 5.5. Their corresponding ultimate moment capacity were determined as 56,212 N-m and 57,610 N-m (41,454 ft-lbs and 42,485 ft-lbs) as shown in Table 7.5. For comparison, one set of TB3-20's, Test 54 to 56, was tested, with the same constant parameters, and their ultimate moment capacity was determined to be 64,920 N-m (47,876 ft-lbs). As can be seen, the two sets of TB3-17's had capacities significantly weaker than the TB3-20 set. On the basis of this experimental test data alone, the replacement of TB1-20's or TB3-20's with TB1-17's or TB3-17's, respectively, cannot be recommended. However, a question more appropriate than are the 431.8 mm (17 inch) t-bases as strong as the 508 mm (20 inch) t-bases might be are the TB1-17's and TB3-17's strong enough to resist any applied forces.

This question can be answered using the ultimate moment capacities predicted by the finite element analyses and the maximum ultimate moment applied to a TB1-17 and a TB3-17. Using values of 21,696 N-m and 29,832 N-m (16,000 ft-lbs and 22,000 ft-lbs), as supplied by TxDOT personnel, as the maximum service load moments applied to a TB1-17 and a TB3-17, respectively, a factor of safety of 1.5 can be applied to obtain the maximum applied ultimate moments of 32,544 N-m and 44,748 N-m (24,000 ft-lbs and 33,000 ft-lbs), respectively.

The standard TxDOT bottom bolt circle is 355.6 mm (14 inches) for any TB1. Using the interpolation computer code developed in this project and a bottom bolt circle of 355.6 mm (14 inches), 2 sets of 2 minimum parameters (d_t and t) were identified which provide adequate strength for a pole diameter between 177.8 and 203.2 mm (7 and 8 inches), inclusive. For d_t equal to 279.4 mm (11.0 inches) and t equal to 31.75 mm (1.25 inches), M_u equals 32,292 N-m (23,814 ft-lbs), and for d_t equal to 292.1 mm (11.5 inches) and t equal to 25.4 mm (1.0 inches), M_u equals 32,484 N-m (23,956 ft-lbs). Even though these two ultimate strength values are slightly less than the ultimate applied moment of 32,544 N-m (24,000 ft-lbs), they are believed to be adequate when 2 factors are considered. First, the finite element values are lower bound values and have additional strength when compared to experimental data. Second, the ultimate strengths of the t-bases were determined in their weakest direction which is 'Door in Diagonal Tension,' (DDT), and the maximum applied moments were determined with the wind forces normal to the luminaire arms. These 2 directions do not normally coincide. If the design wind speed were evaluated at an angle of 45 degrees to the luminaire arms, there would be a reduced surface area and therefore an reduced applied moment. Therefore a TB1-17 can be used to replace a TB1-20 if both the conditions 1 and 2 are satisfied and either condition 3 options are satisfied.

Table 7.4. Comparison of Moment Capacity for TB1-17 and TB1-20
(d_p = 8 in., t = 1.25 in., d_t = 13.5 in., d_b = 15 in.)

Specimen ID	Test ID.	P.O. No.	Breaking Moment (ft.-lb.)	Ultimate Moment for Tested Parameter (ft.-lb.)	Avg. Ultimate Moment for Specimen (ft.-lb.)
TB1-17	TB1-17-5	615643	43,359[a]		42,122
	TB1-17-6	616576	46,230	44,207	
	TB1-17-7		43,131		
	TB1-17-8		34,960[b]		
	TB1-17-9		43,260		
	TB1-17-10	616582	37,610	37,945	
	TB1-17-11		36,440		
	TB1-17-12		39,785		
	TB1-17-13	616544	48,649	44,214	
	TB1-17-14		43,488		
	TB1-17-15		44,410		
	TB1-17-16		40,308		
TB1-20	TB1-20-39	616557	43,506	44,405	44,405
	TB1-20-40		44,830		
	TB1-20-41		44,879		

[a] Only one t-base of this P.O. No. was broken with identical conditions. This test was not used to calculate the average ultimate moment.

[b] This test was not within 10% of the average of tests with same parameters. This test is not included in the average when calculating the ultimate moment for this lot.

Note: 1 inch = 25.4 mm
1 ft-lb = 1.356 N-m

Table 7.5. Comparison of Moment Capacity for TB3-17 and TB3-20
(d_p = 9.5 in., t = 1.25 in., d_t = 15 in., d_b = 17 in.).

Specimen ID	Test ID.	P.O.	Breaking Moment (ft.-lb.)	Ultimate Moment for Tested Parameter (ft.-lb.)	Average Ultimate Moment for Specimen (ft.-lb.)
TB3-17	TB3-17-42	615643	36,704[a]	41,454	41,970
	TB3-17-43		54,140		
	TB3-17-44		47,504[a]		
	TB3-17-45		51,421		
	TB3-17-46		40,153[a]		
	TB3-17-47	616601	43,376	42,485	
	TB3-17-48		41,691		
	TB3-17-49		42,388		
TB3-20	TB3-20-54	612280	48,329	47,876	47,876
	TB3-20-55		47,034		
	TB3-20-56		48,265		

[a] Only lowest three values included in this average, since no three values were within 10% of their average.

Note: 1 inch = 25.4 mm
1 ft-lb = 1.356 mm

1. The pole diameter is between 177.8 and 203.3 mm (7 and 8 inches), inclusive. The bottom bolt circle is 355.6 mm (14 inches), which is the TXDOT standard for model TB1-17
2. Either, the base plate thickness is greater than or equal to 32 mm (1.25 inches) for a minimum top bolt circle of 279.4 mm (11.0 inches) or the base plate thickness is greater than or equal to 25 mm (1.0 inch) for a minimum top bolt circle of 292.1 mm (11.5 inches).

The standard TxDOT bottom bolt circle is 438.15 mm (17.25 inches) for any TB3. Using the interpolation computer code developed in this project and a bottom bolt circle of 431.8 mm (17 inches), which will give conservative results, one minimum parameter is identified for which a TB3-17 will provide adequate strength. For a base plate thickness equal to 32 mm (1.25 inches), a bottom bolt circle equal to 431.8 mm (17.0 inches), a top bolt circle equal to 330.2 mm (13.0 inches), and a pole diameter equal to 203.2 mm (8.0 inches), the ultimate moment capacity is predicted as 46,523 N-m (34,309 ft-lbs) which is above the minimum applied moment of 44,748 N-m (33,000 ft-lbs). A review of the data shows that a TB3-17 can be used to replace a TB3-20 if the base plate thickness is 32 mm (1.25 inches) or greater and if the other 3 parameters are equal to or greater than the minimum values used in this study for TB3-17's.

7.8 Quality Control Study

Several TB1-17 t-bases were bought from different distributors or in different time frames to obtain t-bases from different casting lots and/or heat treating lots to study the effect of material or fabrication variabilities on the ultimate moment capacities of the t-bases. All the dimension parameters were held constant during this phase of this study as given in Table 7.4. The individual breaking moments are also given in Table 7.4 along average breaking moment for each purchase order. Individual TB1-17 breaking moments ranged from 47,406 to 65,968 N-m (34,960 ft-lbs. to 48,649 ft-lbs)., a range of 39% from the lower value. The average moment capacity for each purchase order lot, neglecting any statistical outliers, is also given in Table 7.4. Average purchase order lot moment capacities have a 17% increase from the lowest value.

A similar study was conducted for TB3-17 t-bases. Its dimensional parameters and results are shown in Table 7.5. Individual TB3-17 t-base breaking moments ranged from 49,771 to 73,414 N-m (36,704 ft-lbs. to 54,140 ft.-lbs)., a range of 48% from the lower value. If only the lowest three values of purchase order lot 615643 are used for the average, only a 3% difference is seen between lots. However, if all five values are used there is a 20% difference in purchase order lot averages, a significant difference.

It should also be noted that the failure location for each of the two series, TB1-17 and TB3-17, were randomly distributed between the top and the bottom of the t-bases, further indicating more variability between t-bases.

7.9 Effect of Leveling Devices

Thin u-shaped shims are sometimes placed between the bottom of the t-base and the top of the concrete pier foundation to level the t-base/light pole system and provide a vertical pole. During the initial full scale tests (Test 2 to Test 4), 12.7 mm (0.5 inch) thick washers were place between the t-base and the test frame to account for the effect of the shims. Ultimate moment capacities, see Table 5.3, determined during these 3 tests were much lower than anticipated. Following discussions with TxDOT personnel, pole testing agencies, and the research staff of this project, it was determined that the 12.7 mm (0.5 inch) thick washers over compensated for the thin u-shaped shims sometimes used in the field. It was decided, that in fact, they more closely simulated a double nut leveling device which is not recommended for use with t-bases. The washers were then omitted from Test 5 and the t-base was mounted directly to the steel test frame as was determined to be the more common practice in other t-base tests. The removal of the thick washers resulted in an increase in ultimate moment between 28 % to 54%. This confirms experimentally the weakening effect of the double nut leveling device. The use of the thick washer was suspended for the remainder of the project, and the use of double nut leveling device with t-bases is not recommend.

8. COMPUTER CODE FOR MOMENT CAPACITIES

8.1 Introduction

The experimental and FEM data developed so far is for extreme values of parameters that could be used for connecting t-base with pole base plates and the bottom anchor rods in the pier foundation. In practice, it is necessary to use values that may be in between those used in the experiment as well as in the FEM analysis. The ultimate moment capacity of a t-base could be interpolated for values in between; however since there are four major parameters used in the analysis, the interpolation becomes rather difficult. For this reason, a computer code is developed for the use of the engineer who may have to use parameters that are in between those given here, at the same time used in the filed conditions.

8.2 Interpolation of Ultimate Moment Capacity

The interpolation is made on the assumption that we can possibly use a linear interpolation for parameters in between the ones used. The four parameters changed in the analysis are kept as a constants as the other parameters are altered. If two parameters are used, we have information on a rectangle which is transformed into a square of side 2 varying between -1 to +1. The factors that corresponds to the exact position of a parameter with respect to its extreme limits are computed and using standard techniques for interpolation the corresponding value of the ultimate moment capacity is computed. Here, the concept is extended to four parameters where relevant coefficients are computed based on the location of the field parameter with respect to their corresponding extreme values.

8.3 Computer Code

The Computer code provided here is applicable to both TB1 and TB3 t-bases with 431.8 mm (17 inch) height. The program is an interactive code, in other words, first it will ask whether you want to analyze, TB1 or TB3. For TB1, input 1 and for TB3 input 3 and the computer will automatically collect all the extreme values of the parameters required for the Tb1 and TB3 t-bases. Then the code will ask to input the four parameters in sequence and once the parameters are input, the final interpolated value of the ultimate moment capacity of the t-base will be shown on the computer screen.

The computer code is listed in the appendix.

9. CONCLUSIONS AND RECOMMENDATIONS

9.1 CONCLUSIONS

9.1.1 Variability in T-bases

Variability in the t-base's material properties and geometry effect their ultimate moment capacities. These variabilities come from material non-homogeneity and t-base fabrication processes like casting, welding, and heat treating. The three material properties that were investigated were ultimate tensile strength, modulus of elasticity, and Rockwell Hardness. These values were determined for most of the t-bases tested in this report and their correlation to the t-base's ultimate moment capacity were investigated.

9.1.1.1 Variability in Ultimate Moment Capacities

A significant variation in ultimate moment capacities of t-bases tested with constant dimensional parameters was observed. For t-bases from common purchase orders which assumes common casting and heat treating lots, 32% and 47% increases in ultimate moments capacities were observed for single test values for TB1-17's and TB3-17's, respectively. For t-bases from different purchase orders, multiple test averages were determined for common purchase orders with an increase in ultimate moment capacities of 17% and 3% observed for TB1-17's and TB3-17's, respectively.

9.1.1.2 Variability in Material Properties and Geometry

Ultimate tensile strength, modulus of elasticity, and Rockwell Hardness were determined to all models of t-bases tested, TB1-17, TB1-20, TB3-17, and TB3-20. Three values of each property for each t-base were determined and then averaged for the t-base value. Individual test values are provided in Tables A.1. A.2, and A.3. Average, minimum, and maximum values for each of the four t-base models are provided in Table 5.6. Average material properties of each t-base model were fairly consistent for all material properties determined. However, individual t-base properties increased as much as 44%, 42%, and 135% for ultimate tensile strength, modulus of elasticity, and Rockwell Hardness. A comparison of each material property was made for each t-base against its ultimate moment capacity. No consistent correlation was seen which indicates that geometric variations from casting and welding were also effecting the ultimate moment capacities of the t-bases.

9.1.2 Critical Loading Orientation

Five distinct load orientations are possible with each t-base due to the non-symmetry caused by the door opening on one side of the t-base. To limit the scope of work in this study, an investigation was conducted to determine the weakest direction of load application or the critical load orientation. A review of previous static test data reported by Shrestha (1993) was not conclusive. However, a general trend for the critical load orientation was observed as the moment being applied about an axis parallel to the

diagonal of the t-base top with the door on the tension side. This was designated as, Door in Diagonal Tension (DDT). A finite element study was also completed investigating the five possible load orientations. The finite element analyses showed that DDT produced a maximum principle tensile stress 38% larger than any other load orientation for a constant applied moment of 13,560 N-m (10,000 ft-lbs). This confirmed that DDT was the critical load orientation, and it alone was used for the remainder of this project.

9.1.3 Finite Element Model Validation

Linear finite element models were developed for the TB1-17 and TB3-17 for use in this study. Two methods were used to validate and/or calibrate the models used in this study. First, strains predicted by the finite element model were compared to measured experimental strains. Close correlation was observed for strains in the steel base plate. The degree of correlation for strains in the cast aluminum t-base was dependent on the location in the t-base. A discussion of possible causes for the poorer correlation in the t-base is provided in Chapter 6. Even though the correlation for some locations in the t-base were not as good as hope for, the critical strain locations in the tensile region of the t-base were reasonable and always conservative, yielding a lower bound solution. Second, the ultimate moment capacities of the t-bases with various dimensional parameters were determined experimentally and with finite element analyses. The finite element analyses results were always conservative and again yield a lower bound solution.

9.1.4 Parametric Study of Key Dimensional Parameters

Four key dimensional parameters were identified that were thought to effect the ultimate moment capacity of the t-base. These are the diameters of the bolt circles at the top and bottom of the t-base, the pole base plate thickness, and the pole diameter. Parametric studies were conducted using both full scale experimental testing and finite element analysis. The results of the parametic studies using both methods yielded the same general trends even though the magnitudes of the results varied. Differences in magnitudes of results can be explained since experimental results were effected by variations in material properties and geometry while the finite element models had constant material properties and geometry.

9.1.4.1 Top Bolt Circle

It was observed that the ultimate moment capacities of both t-base models, TB1-17 and TB3-17, increased as the top bolt circle diameter increased with the other parameters held constant. This increase was observed in the finite element analysis and experimental results. The magnitude of the increase was dependent on the magnitude of the other dimensional parameters. The top bolt circle had significant effects on the ultimate moment capacity of the t-base. To maximize the strength of the t-base, the largest top bolt circle should be used.

9.1.4.2 Bottom Bolt Circle

It was observed that the ultimate moment capacities of both t-base models, TB1-17 and TB3-17, increased as the bottom bolt circle diameter increased with the other parameters held constant. This increase was observed in the finite element analysis and experimental results. The magnitude of the increase was dependent on the magnitude of the other dimensional parameters. The bottom bolt circle had significant effects on the ultimate moment capacity of the t-base. To maximize the strength of the t-base, the largest bottom bolt circle should be used.

9.1.4.3 Base Plate Thickness

It was observed that the ultimate moment capacities of both t-base models, TB1-17 and TB3-17, increased as the base plate thickness increased with the other parameters held constant. This increase was observed in the finite element analysis and experimental results. The magnitude of the increase was dependent on the magnitude of the other dimensional parameters. The base plate thickness had moderate effects on the ultimate moment capacity of the t-base. To maximize the strength of the t-base, larger base plate thickness should be used.

9.1.4.4 Pole Diameter

It was observed that the ultimate moment capacities of both t-base models, TB1-17 and TB3-17, increased and decreased as the pole diameter increased with the other parameters held constant. This mixed effect was observed in the finite element analysis and experimental results. The occurrence and magnitude of the increase or decrease was dependent on the magnitude of the other dimensional parameters. The pole diameter had moderate effects on the ultimate moment capacity of the t-base.

9.1.4.5 Interaction of the Key Dimensional Parameters

The effect of any one key dimensional parameter on the magnitude of the ultimate moment capacity of a t-base was always dependent on the magnitude of the other parameters. This confirms the interaction of the key parameters and that all their values must be considered simultaneously when evaluating their effect on the ultimate moment capacity of a t-base. To do this, an interpolation routine was developed to predict the ultimate moment capacity of either t-base model given any set of parameter values which fall within the extreme limits of the parameter values used in this study. This interpolation routine in discussed in Chapter 8.

9.1.5 Comparison of 1975 and 1985 AASHTO Standard T-bases

An experimental study was conducted to compare the strength of t-bases which meet the 1975 and 1985 AASHTO Standards. Both t-base models, TB1 and TB3, were compared. T-bases which meet the 1975 standard are 508 mm (20 inches) in height while those meeting the 1985 standard are 431.8 mm (17 inches) in height. This study was

complete to determine the possibility of direct substitution of 431.8 mm (17 inch) t-bases for 508 mm (20 inch) t-bases in pole knock-down situation. It was determined that both models, TB1-17 and TB3-17, which meet the 1985 AASHTO Standard were had lower ultimate moment capacities than their 1975 counter parts, TB1-20 and TB3-20, and should not be substituted on this basis. Further consideration was given and it was determined that a more appropriate question was, "Not are the newer t-bases as strong as the old t-bases but are the new t-bases strong enough to resist the applied moment?" For the TxDOT supplied maximum service load moments of 21,696 and 32,544 N-m (16,000 and 22,000 ft-lbs) for TB1's and TB3's, respectively, it was determined that the t-bases which meet the 1985 standard could be used to replace t-bases which meet the 1975 standard as long as a combination of minimum values of top bolt circle diameter and base plate thickness are not violated. These minimum values are provide in Chapter 7.

9.1.6 Leveling Devices

It was determined during this study that a double nut leveling device significantly reduces the ultimate moment capacity of the t-base and should not be used. It was observed that the interaction between the bottom flange of the t-base and the supporting material, whether it be a steel test frame or concrete foundation, significantly effects the ultimate moment capacity of the t-base. Step should be taken in the field to insure complete contact between the bottom of the t-base and its supporting material.

9.2 RECOMMENDATIONS

The following recommendations can be made from this study.

1. The load orientation for all future testing and analyses should be limited to "Door in Diagonal Tension," (DDT). This was determined to be the critical load orientation in this study.
2. A minimum of three t-bases should be tested, for any set of parameters and load orientation, and their values averaged when determining an ultimate moment capacity. Previous static test data reviewed typically used only one test for a set of parameters and load orientation.
3. The maximum top and bottom bolt circle diameters should be used to maximize the ultimate moment capacity of the t-base. It should be noted that values for bolt circles less than their maximum can still provided adequate strength yet not their maximum.
4. A thicker base plates increase the ultimate moment capacity of a t-base. A minimum thickness of 25 and 32 mm (1.0 and 1.25 inches) are recommended for TB1-17's and TB3-17's, respectively, to restrict plastic deformations in the base plates.
5. Linear finite element analysis models have been shown to consistently yield lower bound solutions and can be used to predict the ultimate moment capacity of a t-base for a given set of dimensional parameters. A more detailed, complex, nonlinear finite element model could be used to more accurately predict the ultimate moment capacity of a t-base.

6. T-bases which meet the 1975 AASHTO standard can be replaced by t-bases which meet the 1985 AASHTO standard provided that their dimensional parameters are greater than the minimum values identified in Chapter 7, section 7.7 of this report. It was determined in this study that the 1985 t-bases satisfy strength requirements when the identified minimum dimensional parameters limits are satisfied.
7. It was determined that a double nut leveling device significantly reduces the strength of a t-base and should not be used. Care should be taken to insure uniform contact is made between the bottom of the t-base and the foundation support.

APPENDIX A

Table A.1 Average Tensile Strength of Each T-Base

T-Base ID	Purchase Order No.	Tensile Strength, psi			Avg Tensile Strength, psi
		1	2	3	
TB1-17-1	615643	N/A	N/A	N/A	N/A
TB1-17-2	615643	N/A	N/A	N/A	N/A
TB1-17-3		N/A	N/A	N/A	N/A
TB1-17-4		N/A	N/A	N/A	N/A
TB1-17-5	615643	32,600	34,556	33,625	33,593
TB1-17-6	616576	33,606	35,207	34,829	34,547
TB1-17-7		31,681	34,682	33,385	33,249
TB1-17-8		34,085	32,322	33,367	33,258
TB1-17-9		34,500	34,257	34,652	34,469
TB1-17-10	616582	33,327	36,447	33,511	34,428
TB1-17-11		34,256	32,678	31,879	32,937
TB1-17-12		34,386	33,376	30,884[a]	33,881
TB1-17-13	616544	38,149	38,143	38,937	38,409
TB1-17-14		36,388[a]	39,381	35,991	37,686
TB1-17-15		39,108	37,989	39,203	38,766
TB1-17-16		36,494	36,651	33,766[a]	36,572
TB1-17-17	616576	36,461	37,154	38,495	37,370
TB1-17-18		34,841	32,779	32,075	33,231
TB1-17-19		35,091	33,736	33,753	34,193
TB1-17-20		32,347	30,879	30,338	31,188
TB1-17-21	616576	36,672	34,595	35,633	35,633
TB1-17-22		36,187	36,339	35,852	36,126
TB1-17-23		35,953	36,283	37,204	36,480
TB1-17-24	616576	35,166	35,618	34,519	35,101
TB1-17-25		33,299	32,479	32,941	32,906
TB1-17-26		27,320[a]	31,309	32,564[a]	31,309
TB1-17-27	616576	N/A	N/A	N/A	N/A
TB1-17-28		33,516	35,375	33,126	34,005
TB1-17-29		35,697	35,271	32,810[a]	35,484
TB1-17-30	616576	33,183	34,639	33,043	33,621
TB1-17-31	616576	33,256	35,538	33,918	34,237
TB1-17-32		36,384	36,606	34,992	35,994
TB1-17-33		34,595	35,087	32,574	34,085
TB1-17-34		34,086	32,496	32,292	32,958
TB1-17-35	616576	34,305	35,234	34,748	34,762
TB1-17-36		33,125[a]	34,400	37,108[a]	34,400
TB1-17-37		34,285	33,426	34,783	34,164

Table A.1 (Continued) Average Tensile Strength of Each T-Base

T-Base ID		Tensile Strength, psi			Avg Tensile Strength, psi
		1	2	3	
TB1-17-35	616576	34,305	35,234	34,748	34,762
TB1-17-36		33,125[a]	34,400	37,108[a]	34,400
TB1-17-37		34,285	33,426	34,783	34,164
TB1-20-38	616557	N/A	N/A	N/A	N/A
TB1-20-39		33,847	33,594	31,052[a]	33,720
TB1-20-40		31,052	32,355	30,905	31,437
TB1-20-41		32,606	28,454[a]	33,683[a]	32,606
TB3-17-42	615643	32,517	35,053	35,072	34,214
TB3-17-43		28,074[a]	33,289	33,964[a]	33,289
TB3-17-44		35,315	35,993	35,786	35,698
TB3-17-45		34,859	35,571	36,017	35,482
TB3-17-46		27,745[a]	33,356	34,332[a]	33,356
TB3-17-47	616601	32,753	31,439	31,320	31,837
TB3-17-48		31,464	33,269	30,656	31,796
TB3-17-49		36,386	36,555	36,745	36,562
TB3-17-50	616601	35,697	35,037	35,697	35,477
TB3-17-51		34,822	35,080	34,260	34,720
TB3-17-52		35,689	33,763	34,054	34,502
TB3-20-53	612280	N/A	N/A	N/A	N/A
TB3-20-54		34,804	35,743	35,512	35,353
TB3-20-55		37,809	37,863	37,956	37,876
TB3-20-56		34,209	34,540	35,090	34,613
TB3-17-57	616601	35,846	36,113	33,826	35,261
TB3-17-58		34,997	36,619	37,167	36,261
TB3-17-59		37,580	36,007	37,857	37,148
TB3-17-60		35,304	35,230	36,904	35,812
TB3-17-61		35,408	34,319	34,368	34,698

[a] The t-base TB1-17-1 was not broken, hence samples could not be extracted from it.
[b] Test 2 to 4 were conducted with washers between t-base and base plate. Hence these t-bases were not used for material property study.
[c] Tensile strength of this specimen falls outside the ±5% range of the average of the three tests. Hence, it was not used to find the average tensile strength.
[cs] Tensile strength of this specimen falls outside the ±5% range of the average. But the difference is very small. So it is included in the calculation of F_u
[d] The t-bases 27 and 38 were unable to be cut due to their condition.
[e] The TB3-20-53 buckled during the test. Hence, tension test sample could not be extracted from it. Note: 1 psi = 6.895 kPa

Table A.2 Modulus of Elasticity of Each T-Base

T-Base ID	Purchase Order No.	Modulus of Elasticity, psi			Avg Mod. of Elasticity, psi
		1	2	3	
TB1-17-1	615643	N/A	N/A	N/A	N/A
TB1-17-2	615643	N/A	N/A	N/A	N/A
TB1-17-3		N/A	N/A	N/A	N/A
TB1-17-4		N/A	N/A	N/A	N/A
TB1-17-5	615643	8.675E+06	1.001E+07	9.893E+06	9.526E+06
TB1-17-6	616576	1.110E+07	1.080E+07	1.070E+07	1.087E+07
TB1-17-7		1.030E+07	1.070E+07	1.080E+07	1.060E+07
TB1-17-8		1.057E+07	1.165E+07	1.060E+07	1.094E+07
TB1-17-9		1.017E+07	1.140E+07	1.073E+07	1.077E+07
TB1-17-10	616582	1.070E+07	1.050E+07	1.050E+07	1.057E+07
TB1-17-11		1.110E+07	1.060E+07	1.140E+07	1.103E+07
TB1-17-12		1.138E+07	1.163E+07	1.108E+07	1.136E+07
TB1-17-13	616544	1.078E+07	1.100E+07	1.064E+07	1.081E+07
TB1-17-14		1.087E+07	1.110E+07	1.087E+07	1.095E+07
TB1-17-15		1.106E+07	1.085E+07	1.071E+07	1.087E+07
TB1-17-16		1.056E+07	1.047E+07	1.115E+07	1.073E+07
TB1-17-17	616576	1.090E+07	1.040E+07	1.080E+07	1.070E+07
TB1-17-18		9.580E+06	1.130E+07	9.320E+06	1.007E+07
TB1-17-19		1.040E+07	1.110E+07	1.080E+07	1.077E+07
TB1-17-20		1.040E+07	1.030E+07	1.060E+07	1.043E+07
TB1-17-21	616576	9.030E+06	9.210E+06	N/A	9.120E+06
TB1-17-22		9.520E+06	1.200E+07	1.020E+07	1.057E+07
TB1-17-23		8.900E+06	9.320E+06	9.590E+06	9.270E+06
TB1-17-24	616576	1.197E+07	1.158E+07	1.115E+07	1.157E+07
TB1-17-25		1.150E+07	1.080E+07	1.110E+07	1.113E+07
TB1-17-26		1.091E+07	1.073E+07	1.110E+07	1.091E+07
TB1-17-27	616576	N/A	N/A	N/A	N/A
TB1-17-28		1.043E+07	1.064E+07	1.078E+07	1.062E+07
TB1-17-29		1.002E+07	9.945E+06	9.930E+06	9.965E+06
TB1-17-30	616576	9.570E+06	9.640E+06	1.100E+07	1.007E+07
TB1-17-31	616576	1.090E+07	1.120E+07	1.130E+07	1.113E+07
TB1-17-32		1.083E+07	1.115E+07	1.020E+07	1.073E+07
TB1-17-33		1.100E+07	N/A	1.085E+07	1.093E+07

Table A.2 (continued). Modulus of Elasticity of Each T-Base

T-Base ID	Purchase Order No.	Modulus of Elasticity, psi			Avg Mod. of Elasticity, psi
		1	2	3	
TB1-17-34	616576	1.104E+07	1.118E+07	N/A	1.111E+07
TB1-17-35	616576	9.910E+06	1.055E+07	9.863E+06	1.011E+07
TB1-17-36		1.060E+07	1.100E+07	1.070E+07	1.077E+07
TB1-17-37		1.140E+07	1.130E+07	1.070E+07	1.113E+07
TB1-20-38	616557	N/A	N/A	N/A	N/A
TB1-20-39		1.076E+07	1.100E+07	1.133E+07	1.103E+07
TB1-20-40		1.017E+07	1.059E+07	1.098E+07	1.058E+07
TB1-20-41		1.100E+07	9.180E+06	9.470E+06	9.883E+06
TB3-17-42	615643	9.822E+06	9.994E+06	1.010E+07	9.972E+06
TB3-17-43		1.030E+07	1.040E+07	9.750E+06	1.015E+07
TB3-17-44		1.016E+07	1.031E+07	1.015E+07	1.021E+07
TB3-17-45		9.330E+06	9.360E+06	1.030E+07	9.663E+06
TB3-17-46		9.833E+06	1.016E+07	1.012E+07	1.004E+07
TB3-17-47	616601	9.790E+06	9.270E+06	9.990E+06	9.683E+06
TB3-17-48		1.090E+07	1.100E+07	1.150E+07	1.113E+07
TB3-17-49		1.139E+07	1.072E+07	1.041E+07	1.084E+07
TB3-17-50	616601	9.800E+06	9.580E+06	9.830E+06	9.737E+06
TB3-17-51		9.030E+06	8.840E+06	8.050E+06	8.640E+06
TB3-17-52		1.020E+07	1.030E+07	1.040E+07	1.030E+07
TB3-20-53	612280	N/A	N/A	N/A	N/A
TB3-20-54		1.029E+07	1.002E+07	1.063E+07	1.031E+07
TB3-20-55		9.903E+06	1.036E+07	1.033E+07	1.020E+07
TB3-20-56		1.000E+07	1.040E+07	9.251E+06	9.884E+06
TB3-17-57	616601	9.505E+06	9.731E+06	1.060E+07	9.945E+06
TB3-17-58		9.973E+06	1.012E+07	1.014E+07	1.008E+07
TB3-17-59		1.030E+07	1.040E+07	1.050E+07	1.040E+07
TB3-17-60		9.830E+06	9.630E+06	9.180E+06	9.547E+06
TB3-17-61		1.112E+07	1.081E+07	1.057E+07	1.083E+07

Table A.3 Hardness Test results for Transformer Bases

Test ID	Purchase Order No.	Average Hardness
TB1-17-1	615643	N/A
TB1-17-2	615643	N/A
TB1-17-3		N/A
TB1-17-4		N/A
TB1-17-5	615643	N/A
TB1-17-6	616576	41
TB1-17-7		47
TB1-17-8		45
TB1-17-9		50
TB1-17-10	616582	52
TB1-17-11		49
TB1-17-12		49
TB1-17-13	616544	50
TB1-17-14		30
TB1-17-15		31
TB1-17-16		26
TB1-17-17	616576	46
TB1-17-18		50
TB1-17-19		39
TB1-17-20		34
TB1-17-21	616576	48
TB1-17-22		52
TB1-17-23		48
TB1-17-24	616576	52
TB1-17-25		47
TB1-17-26		49
TB1-17-27	616576	N/A
TB1-17-28		N/A
TB1-17-29		N/A
TB1-17-30	616576	N/A

Test ID	Purchase Order No.	Average Hardness
TB1-17-31	616576	45
TB1-17-32		58
TB1-17-33		46
TB1-17-34		49
TB1-17-35	616576	50
TB1-17-36		61
TB1-17-37		48
TB1-20-38	616557	51
TB1-20-39		52
TB1-20-40		43
TB1-20-41		38
TB3-17-42	615643	43
TB3-17-43		42
TB3-17-44		47
TB3-17-45		46
TB3-17-46		49
TB3-17-47	616601	49
TB3-17-48		52
TB3-17-49		55
TB3-17-50	616601	55
TB3-17-51		50
TB3-17-52		49
TB3-20-53	612280	N/A
TB3-20-54		47
TB3-20-55		51
TB3-20-56		38
TB3-17-57	616601	48
TB3-17-58		56
TB3-17-59		55
TB3-17-60		54
TB3-17-61		39

Table A.4 Summary of results from experimental testing and FEM analysis

TEST ID	Moment Capacity ft-lb	Average Moment Capacity ft-lb	FEM Moment Capacity ft-lb	Average Tensile Strength psi	Modulus of Elasticity psi	Rockwell Hardness Number	Purchase Order Number
TB1-17-1	N/A[a]	N/A	N/A	N/A	N/A	N/A	615643
TB1-17-2	28,188[b]			N/A	N/A	N/A	615643
TB1-17-3	33,806[b]	31,557	N/A	N/A	N/A	N/A	615643
TB1-17-4	32,679[b]			N/A	N/A	N/A	615643
TB1-17-5	43,359[c]	43,359	36,565	33,593	9.526E+06	N/A	615643
TB1-17-6	46,230			34,547	1.087E+07	41	616576
TB1-17-7	43,131	44,207	36,565	33,249	1.060E+07	47	616576
TB1-17-8	34,960[d]			33,258	1.094E+07	45	616576
TB1-17-9	43,260			34,469	1.077E+07	50	616576
TB1-17-10	37,610			34,428	1.057E+07	52	616582
TB1-17-11	36,440	37,945	36,565	32,937	1.103E+07	49	616582
TB1-17-12	39,785			33,881	1.136E+07	49	616582
TB1-17-13	48,649			38,409	1.081E+07	50	616544
TB1-17-14	43,488	44,214[e]	36,565	37,253	1.095E+07	30	616544
TB1-17-15	44,410			38,766	1.087E+07	31	616544
TB1-17-16	40,308			36,572	1.073E+07	26	616544
TB1-17-17	31,793			37,370	1.070E+07	46	616576
TB1-17-18	30,739	30,799	24,284	33,231	1.007E+07	50	616576
TB1-17-19	35,471[d]			34,193	1.077E+07	39	616576
TB1-17-20	29,864			31,188	1.043E+07	34	616576
TB1-17-21	38,200			35,633	9.120E+06	48	616576
TB1-17-22	39,138	39,669	35,340	36,126	1.057E+07	52	616576
TB1-17-23	41,669			36,480	9.270E+06	48	616576
TB1-17-24	45,027			35,101	1.157E+07	52	616576
TB1-17-25	44,525	44,639	39,680	32,906	1.113E+07	47	616576
TB1-17-26	44,366			31,309	1.091E+07	49	616576
TB1-17-27	32,409			N/A	N/A	N/A	616576
TB1-17-28	30,478	30,944	24,012	34,005	1.062E+07	N/A	616576
TB1-17-29	29,946			35,484	9.965E+06	N/A	616576
TB1-17-30	29,945	29,945[f]	21,937	33,621	1.007E+07	N/A	616576
TB1-17-31	37,316			34,237	1.113E+07	45	616576
TB1-17-32	31,210[d]	37,971	30,864	35,994	1.073E+07	58	616576
TB1-17-33	38,776			34,085	1.093E+07	46	616576
TB1-17-34	37,820			32,958	1.111E+07	49	616576
TB1-17-35	40,873			34,762	1.011E+07	50	616576
TB1-17-36	39,931	40,697	29,242	34,400	1.077E+07	61	616576
TB1-17-37	41,286			34,164	1.113E+07	48	616576

Table A.4 (continued). Summary of results from experimental testing and FEM analysis

TEST ID	Moment Capacity ft-lb	Average Moment Capacity ft-lb	FEM Moment Capacity ft-lb	Average Tensile Strength psi	Modulus of Elasticity psi	Rockwell Hardness Number	Purchase Order Number
TB1-20-38	33,524[d]			N/A	N/A	51	616557
TB1-20-39	43,506	44,405	N/A	33,720	1.103E+07	52	616557
TB1-20-40	44,830			31,437	1.058E+07	43	616557
TB1-20-41	44,879			32,606	9.883E+06	38	616557
TB3-17-42	36,704[g]			34,214	9.972E+06	43	615643
TB3-17-43	54,140			33,289	1.015E+07	42	615643
TB3-17-44	47,504[g]	41,453	38,935	35,698	1.021E+07	47	615643
TB3-17-45	51,421			35,482	9.663E+06	46	615643
TB3-17-46	40,153[g]			33,356	1.004E+07	49	615643
TB3-17-47	43,376			31,837	9.683E+06	49	616601
TB3-17-48	41,691	42,485	38,935	31,796	1.113E+07	52	616601
TB3-17-49	42,388			36,562	1.084E+07	55	616601
TB3-17-50	34,749			35,477	9.737E+06	55	616601
TB3-17-51	35,121	35,034	27,736	34,720	8.640E+06	50	616601
TB3-17-52	35,234			34,502	1.030E+07	49	616601
TB3-20-53	52,684[h]			N/A	N/A	N/A	612280
TB3-20-54	48,329	47,876	N/A	35,353	1.031E+07	47	612280
TB3-20-55	47,034			37,876	1.020E+07	51	612280
TB3-20-56	48,265			34,613	9.884E+06	38	612280
TB3-17-57	53,296[d]			35,261	9.945E+06	48	616601
TB3-17-58	45,234			36,261	1.008E+07	56	616601
TB3-17-59	48,792	45,665	44,950	37,148	1.040E+07	55	616601
TB3-17-60	42,880			35,812	9.547E+06	54	616601
TB3-17-61	53,261[d]			34,698	1.083E+07	39	616601

[a] This test was used to compare experimental strain readings to FEM strain readings

[b] Tests 2 to 4 were done with washers (O.D.=2.75 in., Thk=0.5 in.) in between T-Base bottom and test frame at four corners of the T-base.

[c] Test 5 was done without any washer in between T-base bottom and test frame to check the difference in breaking moment

[d] Breaking moment from this test was not within 10% of the average of tests with the same test parameters.

[e] Four tests were used to calculate the ultimate moment

[f] Only one test was done with this parameter. The base plate bent 0.5 inch and its reuse was not possible.

[g] Moment capacity from all five tests for TB3-17 with P.O.no. 615643 differed by more than 10% from the average. So lower three test results were considered to calculate the average.

[h] This TB3-20 sample showed buckling phenomena during loading. It started buckling at 52,684 ft-lb moment and it cracked only during unloading at same location of buckling.

Note: 1 psi = 6.895 kPa 1 ft-lb = 1.356 N-m 1 inch = 25.4 mm

APPENDIX B

```
C     INT.FOR This program is used to interpolate a function
C     in FOUR-dimensions
      DIMENSION R(16),S(16),T(16),U(16),TB1(88),TB3(88)
      DIMENSION X(16),Y(16),Z(16),A(16),P(16)

      DATA R/ -1.,1.,1.,-1.,-1.,1.,1.,-1.,-1.,1.,1.,-1.,-1.,1.,1.,-1./
      DATA S/ -1.,-1.,1.,1.,-1.,-1.,1.,1.,-1.,-1.,1.,1.,-1.,-1.,1.,1./
      DATA T/ -1.,-1.,-1.,-1.,1.,1.,1.,1.,-1.,-1.,-1.,-1.,1.,1.,1.,1./
      DATA U/ -1.,-1.,-1.,-1.,-1.,-1.,-1.,-1.,1.,1.,1.,1.,1.,1.,1.,1./
      DATA TB1/7.,1.,11.,13.,22971,8.,1.,11.,13.,21819,
     * 8.,1.5,11.,13.,24870,7.,1.5,11.,13.,24747,7.,1.,13.5,13.,30830,
     * 8.,1.,13.5,13.,29196,8.,1.5,13.5,13,29288,7.,1.5,13.5,13,30899,
     * 7.,1.,11.,15.,23310,8.,1.,11.,15.,21937,8.,1.5,11.,15.,26630,
     * 7.,1.5,11.,15.,40632,7.,1.,13.5,15.,38727,8.,1.,13.5,15.,35340,
     * 8.,1.5,13.5,15.,37790,7.,1.5,13.5,15.,40632,7.,8.,1,1.5,
     * 11.,13.5,13.,15./
      DATA TB3/8.,1.,13.,15.,24810,10.,1.,13.,15.,25352,
     * 10.,1.5,13.,15.,25548,8.,1.5,13.,15.,25745,8.,1.,15.,15.,31406,
     * 10.,1.,15.,15.,26176,10.,1.5,15.,15,26410,8.,1.5,15.,15.,32720,
     * 8.,1.,13.,17.,30975,10.,1.,13.,17.,31104,10.,1.5,13.,17.,43435,
     * 8.,1.5,13.,17.,37643,8.,1.,15.,17.,33209,10.,1.,15.,17.,32824,
     * 10.,1.5,15.,17.,45716,8.,1.5,15.,17.,42652,8.,10.,1,1.5,
     * 13.,15.,15.,17./
      DIS = 'INCH'
      CM1 = 'FT-'
      CM2 = 'LBS'
      write (*,*) 'Input 1 for TB1 and 2 for TB3 Analysis'
      READ (5,*) KON
      IF (KON.EQ.2) GO TO 120
C     READ (5,*) TYPE
C     IF (TYPE.EQ.'TB3') GO TO 120

      DO 100 I = 1, 16
      K = 5 * I - 4
      X(I) = TB1(K)
      Y(I) = TB1(K+1)
      Z(I) = TB1(K+2)
      A(I) = TB1(K+3)
      P(I) = TB1(K+4)
  100 CONTINUE
      XMIN = TB1(81)
      XMAX = TB1(82)
      YMIN = TB1(83)
      YMAX = TB1(84)
      ZMIN = TB1(85)
      ZMAX = TB1(86)
      AMIN = TB1(87)
      AMAX = TB1(88)
      GO TO 130
  120 DO 125 I = 1, 16
      K = 5 * I - 4
      X(I) = TB3(K)
      Y(I) = TB3(K+1)
      Z(I) = TB3(K+2)
```

```
      A(I) = TB3(K+3)
      P(I) = TB3(K+4)
  125 CONTINUE
      XMIN = TB3(81)
      XMAX = TB3(82)
      YMIN = TB3(83)
      YMAX = TB3(84)
      ZMIN = TB3(85)
      ZMAX = TB3(86)
      AMIN = TB3(87)
      AMAX = TB3(88)
  130 write (*,*) 'Input diameter of the pole'
      WRITE (*,10) XMIN, XMAX, DIS
   10 FORMAT (/' This value must be in between',F7.2,' AND',F7.2,A5/)
      read (*,*) xi
      write (*,*) 'Input thickness of the base plate'
      WRITE (*,10) YMIN, YMAX, DIS
      read (*,*) yi
      write (*,*) 'Input top bolt circle diameter'
      WRITE (*,10) ZMIN, ZMAX, DIS
      read (*,*) zi
      write (*,*) 'Input bottom bolt circle diameter'
      WRITE (*,10) AMIN, AMAX, DIS
      read (*,*) ai
      RI = 2.*(XI - XMIN)/(XMAX -XMIN) - 1.
      SI = 2.*(YI - YMIN)/(YMAX -YMIN) - 1.
      TI = 2.*(ZI - ZMIN)/(ZMAX -ZMIN) - 1.
      UI = 2.*(AI - AMIN)/(AMAX -AMIN) - 1.
C     WRITE (*,*) XI, YI,ZI, AI, RI, SI,TI,UI
      WRITE (*,15) XI,dis, YI,dis,ZI,dis, AI,dis
   15 FORMAT (/' Diameter of the Steel Pole.........=',F10.2,A5/
     *        ' Thickness of the Base Plate........=',F10.2,A5/
     *        ' Top Bolt Circle Diameter...........=',F10.2,A5/
     *        ' Bottom Bole Circle Diameter........=',F10.2,A5//)
      PI = 0.
      DO 200 I = 1,16
  200 PI = PI + (1.+RI*R(I))*(1.+SI*S(I))*(1.+TI*T(I)) *
     *    (1.+UI*U(I)) * P(I)/16.
      IF (KON.EQ.2) WRITE (*,*) 'This is for TB3-17 T-Base'
      IF (KON.EQ.1) WRITE (*,*) 'This is for TB1-17 T-Base'
   16 FORMAT (/' Ultimate moment capacity...........=',F15.1,A6,A3//)
      WRITE (*,16) PI,CM1,CM2
      STOP
      END
```